

42



**INFLUENCE OF INITIAL BOUNDARY LAYER
ON THE TWO-DIMENSIONAL TURBULENT MIXING
OF A SINGLE STREAM**

R. C. Bauer and R. J. Matz

ARO, Inc.

April 1971

Approved for public release; distribution unlimited.

**ENGINE TEST FACILITY
ARNOLD ENGINEERING DEVELOPMENT CENTER
AIR FORCE SYSTEMS COMMAND
ARNOLD AIR FORCE STATION, TENNESSEE**

NOTICES

When U. S. Government drawings specifications, or other data are used for any purpose other than a definitely related Government procurement operation, the Government thereby incurs no responsibility nor any obligation whatsoever, and the fact that the Government may have formulated, furnished, or in any way supplied the said drawings, specifications, or other data, is not to be regarded by implication or otherwise, or in any manner licensing the holder or any other person or corporation, or conveying any rights or permission to manufacture, use, or sell any patented invention that may in any way be related thereto.

Qualified users may obtain copies of this report from the Defense Documentation Center.

References to named commercial products in this report are not to be considered in any sense as an endorsement of the product by the United States Air Force or the Government.

INFLUENCE OF INITIAL BOUNDARY LAYER
ON THE TWO-DIMENSIONAL TURBULENT MIXING
OF A SINGLE STREAM

R. C. Bauer and R. J. Matz
ARO, Inc.

Approved for public release; distribution unlimited.

FOREWORD

The work reported herein was sponsored by Headquarters, Arnold Engineering Development Center (AEDC), Air Force Systems Command (AFSC), Arnold Air Force Station, Tennessee, in support of Program Element 62302F, Project 5730.

The results of research presented were obtained by ARO, Inc. (a subsidiary of Sverdrup & Parcel and Associates, Inc.), contract operator of AEDC, AFSC, under Contract F40600-71-C-0002. The exact numerical solution outlined in this report was developed under ARO Projects No. RW2608 and RW5711. Initial results from the exact solution were presented to the November 1968 Project Squid Workshop on Turbulent Transport Properties in Chicago, Illinois. The simplified approximate solution was developed under ARO Projects No. RW5807 and RW5905. The manuscript for this report was submitted for publication on February 9, 1971.

This technical report has been reviewed and is approved.

Eules L. Hively
Research and Development Division
Directorate of Technology

Harry L. Maynard
Colonel, USAF
Director of Technology

ABSTRACT

An integral method is presented for estimating the influence of an initial boundary layer on the development of a two-dimensional, isobaric, turbulent, free shear layer. The basic equation is derived by applying the principle that, at any streamwise station along the free shear layer, the momentum of the entrained flow equals the total axial turbulent shear force acting along the dividing streamline. This equation is solved using a single parameter family of velocity profiles derived by Korst and Prandtl's mixing length concept for turbulent shear stress. The theory involves one empirical constant which was evaluated using Tollmien's experimental data for incompressible, turbulent mixing. The theory is verified by comparing with experimental data for free-stream Mach numbers up to 6.4.

CONTENTS

	<u>Page</u>
ABSTRACT	iii
NOMENCLATURE	vi
I. INTRODUCTION	1
II. BASIC EQUATIONS	1
III. NUMERICAL TECHNIQUES	5
IV. EXPERIMENTAL VERIFICATION	7
V. CONCLUSIONS	8
REFERENCES	9

APPENDIXES

I. ILLUSTRATIONS

Figure

1. General Mixing Zone	13
2. Typical Family of Velocity Profiles	14
3. Comparison of Theory and Chapman's Data	
a. $\psi = 2.0$, $M_\infty = 0.19$	15
b. $\psi = 3.3$, $M_\infty = 0.19$	16
c. $\psi = 4.7$, $M_\infty = 0.19$	17
d. $\psi = 9.7$, $M_\infty = 0.19$	18
4. Comparison of Theory and Hill's Data	
a. $\psi = 2.1$, $M_\infty = 2.1$	19
b. $\psi = 4.6$, $M_\infty = 2.1$	20
c. $\psi = 8.4$, $M_\infty = 2.1$	21
d. $\psi = 17.4$, $M_\infty = 2.1$	22
e. $\psi = 4.3$, $M_\infty = 2.5$	23
f. $\psi = 7.7$, $M_\infty = 2.5$	24
g. $\psi = 16.0$, $M_\infty = 2.5$	25
5. Comparison of Theory and High-Speed Data from Ref. 9	
a. $\psi = 2.7$, $M_\infty = 4.0$	26
b. $\psi = 13.3$, $M_\infty = 4.0$	27
c. $\psi = 3.33$, $M_\infty = 6.4$	28
d. $\psi = 15.8$, $M_\infty = 6.4$	29
6. Theoretical Variation of Dividing Streamline Friction Coefficient	30

<u>Figure</u>		<u>Page</u>
7.	Theoretical Variation of Mixing Length Proportionality Constant	31
8.	Comparison of Theoretical Mixing Growth	
a.	With Chapman's Data	32
b.	With Hill's Data	33
II.	EQUATIONS FOR THE CHARACTERISTICS OF GENERAL, SINGLE-STREAM MIXING ZONES	34

NOMENCLATURE

b	Width of mixing zone (Fig. 1)
C	Crocco number
C_f	Coefficient of friction, $\frac{r}{\frac{\rho_\infty u_\infty^2}{2}}$
F	Total force
G	Net mass flow
I, J	Integral quantities, defined as follows:

$$I_1 = \int_{-\eta_M}^{\eta} \frac{\phi}{\frac{T_t}{T_{t_\infty}} - C_\infty^2 \phi^2} d\eta, \quad I_3 = \int_{-\eta_M}^{\eta} \frac{\phi^2}{\frac{T_t}{T_{t_\infty}} - C_\infty^2 \phi^2} d\eta$$

$$J_1 = \int_{-\eta_M}^{\eta} \frac{\phi}{\frac{T_t}{T_{t_\infty}} - C_\infty^2 \phi^2} \eta d\eta, \quad J_3 = \int_{-\eta_M}^{\eta} \frac{\phi^2}{\frac{T_t}{T_{t_\infty}} - C_\infty^2 \phi^2} \eta d\eta$$

k	Ratio of Prandtl's mixing length to mixing zone width
l	Prandtl's mixing length
M	Mach number
p	Base pressure and static pressure throughout mixing zone and inviscid flow field
R	Gas constant
r	Radius from axis of symmetry to inviscid jet boundary (Appendix II)

T	Static temperature
T_t	Total temperature
u	Velocity
X	Streamwise intrinsic coordinate (Fig. 1)
Y	Transverse intrinsic coordinate (Fig. 1)
y	Transverse coordinate of initial boundary layer
β	Dummy variable in Eq. (5)
γ	Ratio of specific heats
δ	Thickness of initial boundary layer (Fig. 1)
η	Non-dimensional mixing ordinate, $\frac{\sigma Y}{X}$
θ	Momentum thickness of initial boundary layer, Eq. (13) or angle between coordinate reference line and axis of symmetry (Appendix II)
ρ	Density
σ	Local similarity parameter
τ	Viscous shear stress
ϕ	Velocity ratio, $\frac{u}{u_\infty}$
ψ	Non-dimensional intrinsic streamwise distance, $\frac{X}{\delta}$

SUBSCRIPTS

b	Base region (Fig. 1)
D	Dividing streamline
FD	Fully developed mixing
I	Inviscid
i	Initial boundary layer
M	Extremities of mixing region (Fig. 1)
m	Inviscid jet boundary (Fig. II-1)
P	Position parameter
t	Total or stagnation condition

V	With mixing
w	Wall (Fig. 1)
∞	Free stream
3	Station 3 conditions (Fig. II-1)

SECTION I INTRODUCTION

The influence of an initial boundary layer on the development of a turbulent free shear layer is an important factor in the analysis of separated flows as well as in the basic study of turbulent mixing processes. Historically, the initial boundary layer is treated by the "displaced origin" technique which accounts for the increased size of the far field mixing zone, but does not predict the evolution of the velocity profile. Hill (Ref. 1) has refined the displaced origin technique and is able to predict the evolution of the velocity profile. He verifies his technique by comparing with more exact theoretical results for laminar mixing and experimental results for turbulent mixing. For turbulent mixing, Hill assumes a linear variation of eddy viscosity with distance and accounts for compressibility effects with the Donaldson and Gray correlation. Lamb (Ref. 2) determines the evolution of velocity profile in a turbulent mixing zone by using the transverse momentum equation to determine the eddy viscosity. This technique has not been extensively verified by experiment and will not predict a laminar mixing process because use of the transverse momentum equation results in an overspecification of the problem.

The integral method developed by Bauer (Ref. 3) has been extended by Willbanks (Ref. 4) and applied to laminar mixing with an initial boundary layer. Willbanks verifies his technique by comparing with more exact theoretical results for laminar mixing. In this report, the method of Ref. 4 is applied to the case of turbulent mixing with an initial boundary layer.

SECTION II BASIC EQUATIONS

A sketch of the type of mixing considered is shown in Fig. 1 (Appendix I). The conservation of momentum condition is applied to the control volume shown in Fig. 1 based on the following assumptions:

1. Over the mixing zone length considered (X), the average angle between the dividing streamline and the mixing zone centerline is small (<20 deg).
2. The mixing is two-dimensional, isobaric, and constant composition.

The momentum equation for this control volume is

$$\int_0^X \tau_D dX = \int_{-Y_M}^{Y_D} \rho u^2 dY \quad (1)$$

Equation (1) is written in terms of the intrinsic coordinate system introduced by Chapman and Korst in Ref. 5. The intrinsic coordinate system results from far-reaching simplifications of the equation of motion which is reduced to the form of the heat conduction equation for non-steady, one-dimensional heat flow. Solutions to this highly simplified equation of motion must be interpreted in terms of a coordinate system (intrinsic) which is shifted relative to the usual inviscid flow coordinate system. The location of the intrinsic coordinate system can be determined by applying the conservation of total momentum condition (Appendix II).

By using the perfect gas law,

$$\rho = \frac{P}{RT} = \frac{P}{RT_{t\infty} \left(\frac{T_t}{T_{t\infty}} - C_\infty^2 \phi^2 \right)}$$

where

$$\phi = \frac{u}{u_\infty}$$

and

$$C_\infty^2 = 1 - \left(\frac{T_\infty}{T_{t\infty}} \right)$$

and by using the transformation,

$$\eta = \frac{\sigma Y}{X}$$

where σ is the local similarity parameter and is a function of both C_∞ and X , substitution into Eq. (1) yields

$$\int_0^X \tau_D dX = \rho_\infty u_\infty^2 (1 - C_\infty^2) \left(\frac{X}{\sigma} \right) \int_{-\eta_M}^{\eta_D} \frac{\phi^2}{\frac{T_t}{T_{t\infty}} - C_\infty^2 \phi^2} d\eta \quad (2)$$

In the above transformation, σ is the local similarity parameter as introduced by Chapman and Korst (Ref. 5). The local similarity parameter is a function of both C_∞ and X and asymptotically approaches the well-known Goertler parameter as $X \rightarrow \infty$.

If a coefficient of friction is defined as follows

$$C_{fD} = \frac{r_D}{\left(\frac{\rho_\infty v_\infty^2}{2}\right)}$$

with

$$\psi = \frac{x}{\delta}$$

$$(I_3)_{\eta_D} = \int_{-\eta_M}^{\eta_D} \frac{\phi^2}{\frac{T_t}{T_{t_\infty}} - C_\infty^2 \phi^2} d\eta$$

and

$$\eta_P = \frac{\sigma \delta}{X} = \frac{\sigma}{\psi} \quad (3)$$

then substitution into Eq. (2) yields

$$\int_0^\psi C_{fD} d\psi = \frac{2}{\eta_P} (1 - C_\infty^2) (I_3)_{\eta_D} \quad (4)$$

Equation (4) is the basic momentum equation and applies for either laminar or turbulent mixing. To solve Eq. (4), it is necessary to specify C_{fD} in terms of X and η_P , and it is necessary to describe a family of velocity profiles with η_P as a parameter. The desired family of velocity profiles was derived by Chapman and Korst in Ref. 5. The equation is as follows:

$$\phi = \frac{1}{2} [1 + \operatorname{erf}(\eta - \eta_P)] + \frac{1}{\sqrt{\pi}} \int_{\eta - \eta_P}^{\eta} \left[\phi_i \left(\frac{\eta - \beta}{\eta_P} \right) \right] e^{-\beta^2} d\beta \quad (5)$$

Equation (5) may be regarded as an interpolation equation between the initial boundary layer $\phi_i \left(\frac{\eta - \beta}{\eta_P} \right)$ and a fully developed mixing velocity profile given by $1/2 (1 + \operatorname{erf} \eta)$ for corresponding variations in η_P from infinity to zero. A typical family of velocity profiles is presented in Fig. 2.

In this report, only turbulent mixing is considered, and Prandtl's mixing length hypothesis is used to define the coefficient of friction (C_{f_D}). By definition,

$$C_{f_D} = \frac{\tau_D}{\left(\frac{\rho_\infty v_\infty^2}{2}\right)} \quad (6)$$

Prandtl's mixing length hypothesis, as it is applied in this report yields

$$\tau_D = \rho_D \ell_D^2 \left(\frac{\partial u}{\partial Y}\right)_D^2$$

or in non-dimensional form

$$\frac{\tau_D}{\left(\frac{\rho_\infty v_\infty^2}{2}\right)} = \frac{2\ell_D^2 (1 - C_\infty^2)}{\left(\frac{T_{tD}}{T_{t\infty}} - C_\infty^2 \phi^2\right)} \left(\frac{\sigma}{X}\right)^2 \left(\frac{d\phi}{d\eta}\right)_D^2 \quad (7)$$

The usual assumption concerning the mixing length ℓ_D is (Ref. 6)

$$\ell_D = kb \quad (8)$$

where k is a non-dimensional empirical parameter and b is an arbitrarily defined width of the mixing region (Fig. 1). The coordinate η_b is defined by

$$b = \eta_b \left(\frac{X}{\sigma}\right) \quad (9)$$

where η_b is the corresponding non-dimensional width of the mixing region. Since the non-dimensional velocity profile [Eq. (5)] is a function of X , then η_b will also be a function of X .

Substituting Eq. (9) into Eq. (8) yields

$$\ell_D = \eta_b k \left(\frac{X}{\sigma}\right) \quad (10)$$

As in Ref. 3, k is assumed to be independent of free-stream Mach number, and in addition, it is further assumed that the product $\eta_b k$ is independent of X . The latter assumption specifies the functional relation between k and X to be the inverse of the functional relation between η_b and X . These relationships are predicted by the theory since the combined assumptions allow the product $\eta_b k$ to be determined from a single experiment. The validity of these assumptions will be established by comparison with experimental results.

The coefficient of friction is obtained by substituting Eqs. (10) and (7) into Eq. (6); therefore,

$$C_{f_D} = \frac{2(\eta_b k)^2 (1 - C_\infty^2)}{\frac{T_{t_D}}{T_{t_\infty}} - C_\infty^2 \phi^2} \left(\frac{d\phi}{d\eta} \right)_D \quad (11)$$

The total temperature distribution through the mixing zone and initial boundary layer was determined from the well-known Crocco relation for unity Prandtl number. Application of the Crocco relation assumes an instantaneous change in the total temperature distribution at the separation point, which of course is not true. Therefore, only moderate total temperature differences are adequately approximated by the Crocco relation. The location of the dividing streamline was determined by the method discussed in Appendix II, which was developed for the more general case of axisymmetric mixing. The equation is

$$\int_{-\infty}^{\eta_D} \frac{\phi}{\frac{T_t}{T_{t_\infty}} - C_\infty^2 \phi^2} d\eta = \int_{-\infty}^{\infty} \frac{(\phi - \phi^2)}{\frac{T_t}{T_{t_\infty}} - C_\infty^2 \phi^2} d\eta - \left(\frac{\eta_P}{1 - C_\infty^2} \right) \left(\frac{\theta}{\delta} \right) \quad (12)$$

where θ is the momentum thickness of the initial boundary layer defined by the following equation:

$$\frac{\theta}{\delta} = (1 - C_\infty^2) \int_0^{1.0} \frac{(\phi_i - \phi_i^2)}{\frac{T_{t_i}}{T_{t_\infty}} - C_\infty^2 \phi_i^2} d\left(\frac{y}{\delta}\right) \quad (13)$$

Sufficient information is now available for the numerical solution of Eq. (4) for a specified initial boundary layer.

SECTION III NUMERICAL TECHNIQUES

3.1 EXACT SOLUTION

The numerical technique used to solve Eq. (4) is the method of finite differences based on the following conditions at $\psi = 0$,

$$\eta_P = \infty \quad \text{and} \quad C_{f_D} = 0$$

Various values of η_P were selected starting in the range from 6.0 to 10.0 and decreasing to zero in increments of 0.1 to 0.5. This calculation

yields η_P as a function of ψ . The velocity profile can then be determined at each value of ψ from Eq. (5) and transformed into physical coordinates by the following equation:

$$\frac{\eta}{\eta_P} = \frac{Y}{\delta}$$

It is interesting to note that the similarity parameter (σ) is not required in the transformation to the physical plane except for the case of fully developed mixing which occurs when $\psi = \infty$ and $\eta_P = 0$. The variation of the local similarity parameter (σ) with ψ can be determined from Eq. (3).

This numerical technique was programmed on an IBM 360/50 computer, and a typical calculation time is approximately 1 min for each value of η_P considered or about 15 min for a complete mixing process.

3.2 APPROXIMATE SOLUTION

Experience with the exact numerical solution has led to the development of an approximate solution which can be very useful in solving practical engineering problems. The approximate solution is obtained by integrating the left hand side of Eq. (4) by parts. This yields the following

$$\int_0^{\psi} C_{fD} d\psi = C_{fD} \psi - \int_0^{\psi} \psi \left(\frac{dC_{fD}}{d\psi} \right) d\psi \quad (14)$$

The integral on the right-hand side of Eq. (14) can be neglected for the following two reasons:

1. Experience with the exact solution shows that $\frac{dC_{fD}}{d\psi} \approx 0$ for $\psi \geq 10$.
2. For $\psi < 10$, the exact solution underestimates the value of the integral appearing on the left-hand side of Eqs. (4) and (14) relative to its true physical value because of the boundary condition $C_{fD} = 0$ and $\psi = 0$. This boundary condition implies that, at the separation point, the shear stress varies discontinuously from that produced by the initial boundary layer to zero. This is physically unrealistic, and therefore, the error produced by neglecting the integral on the right-hand side of Eq. (14) results in a more realistic estimate of the integral for total shear.

Based on these arguments, Eq. (4) can be written in the following approximate form:

$$C_{f_D} \psi = \frac{2(1 - C_\infty^2)}{\eta_P} (I_3) \eta_D \quad (15)$$

With Eq. (15), it is possible to calculate the properties of the mixing process at any given station (ψ) without the need for calculating the complete mixing process up to that station. The local similarity parameter (σ) can then be determined from Eq. (3). A typical calculation time on an IBM 360/50 computer is less than one minute.

SECTION IV EXPERIMENTAL VERIFICATION

The theory developed in the previous section involves one constant ($\eta_P k$) to be determined from experiment. The experiment selected is that of Tollmien (Ref. 7) for incompressible ($C_\infty^2 \approx 0$), fully developed, turbulent mixing. Tollmien experimentally determines a value of 12 for the similarity parameter (σ) which results in a value of 0.2058 for $\eta_P k$. By using this constant, the theory is compared with available two-dimensional data in Figs. 3, 4, and 5.

To facilitate the comparison of velocity profile shape and size, the transverse location of the theoretical profiles was determined by matching their half-velocity point with the experimental. However, it is possible to theoretically locate the velocity profiles by the method presented in Appendix II. The theory, evaluated either by the exact or approximate method, is shown to predict reasonable well both the evolution of velocity profile shape and the size of the mixing zone for free-stream Mach numbers up to 6.4. As anticipated, the approximate method is more realistic than the exact method for values of $\psi < 10$. A basic assumption in the development of the approximate method is that $\frac{dC_{f_D}}{d\psi} = 0$ for $\psi > 10$. This assumption is verified by the plot of C_{f_D} versus ψ presented in Fig. 6.

The basic assumption in this analysis is that the product ($\eta_P k$) is a constant which is independent of both free-stream Mach number and mixing distance (X). Based on this assumption, it is possible to determine the variation with X of the constant of proportionality (k) between

the mixing length (ℓ) and a selected mixing width (b). A typical variation of k with ψ is presented in Fig. 7 for a mixing zone width defined by the velocity ratios 0.9845 and 0.0154.

The influence of an initial boundary layer on the width of a turbulent mixing zone is presented in Figs. 8a and b for incompressible flow (Chapman's data, Ref. 5) and for supersonic flow (Hill's data, Ref. 1). Theoretical estimates are included based on the exact and approximate solution techniques and for fully developed turbulent mixing without an initial boundary layer. Again, the approximate solution is shown to agree better with experiment than with the exact solution.

SECTION V CONCLUSIONS

Analysis of the development of a two-dimensional, isobaric, constant composition, compressible, free turbulent shear layer from an initial boundary layer leads to the following conclusions:

1. The velocity profile becomes essentially fully developed in a streamwise distance corresponding to about ten initial boundary layer thicknesses.
2. The near field local mixing rate varies significantly in the first ten initial boundary layer thicknesses. The experimental data considered in this report are too limited to establish the far field or fully developed mixing rate.
3. The theory presented in this report has been verified for the near field mixing process.
4. The analytical technique presented in this report becomes impractical when applied to mixing processes that are strongly influenced by axisymmetric effects. The complexity introduced by axisymmetric effects is primarily in connection with the determination of the location of the dividing streamline. A typical example is presented in Appendix II. For the more complex mixing processes, numerical techniques (Ref. 10) are believed to be superior in both phenomenological representation and computation time.

REFERENCES

1. Hill, W. G. "Initial Development of Compressible Turbulent Free Shear Layers." Ph. D Thesis, Rutgers, May 1966.
2. Lamb, J. P. "An Approximate Theory for Developing Turbulent Free Shear Layers." Journal of Basic Engineering, September 1967, pp. 633-640.
3. Bauer, R. C. "An Analysis of Two-Dimensional Laminar and Turbulent Compressible Mixing." AIAA Journal, Vol. 4, No. 3, March 1966, pp. 392-395.
4. Willbanks, C. E. "An Integral Analysis of the Compressible Laminar Free Shear Layer." Fourth Annual Southeastern Seminar on Thermal Sciences, May 20-21, 1968.
5. Chapman, A. J., Korst, H. H. "Free Jet Boundary with Consideration of Initial Boundary Layer." Second U. S. National Congress of Applied Mechanics, June 14-18, 1954.
6. Hinze, J. O. Turbulence. McGraw-Hill, New York, 1959.
7. Tollmien, W. "Calculation of Turbulent Expansion Processes." NACA TM-1085, translated by J. Vanier, 1945.
8. Chapman, A. J. "Mixing Characteristics of a Free Jet Boundary with Consideration of Initial Boundary Layer Configuration." Ph. D Thesis, University of Illinois, 1953.
9. Lamb, J. P. and Bass, R. L. "Some Correlations of Theory and Experiment for Developing Turbulent Free Shear Layers." Paper No. 68-FE-9 Presented at the ASME Fluids Engineering Conference, Philadelphia, Pennsylvania, May 6-8, 1968.
10. Lee, S. C. and Harsha, P. T. "The Use of Turbulent Kinetic Energy in Free Mixing Studies." AIAA 2nd Fluid and Plasma Dynamic Conference, June 1969.
11. Zumwalt, G. W. "Analytical and Experimental Study of the Axially Symmetric Supersonic Base Pressure Problem." Ph. D Thesis, University of Illinois, 1959.
12. Bauer, R. C. "Characteristics of Axisymmetric and Two-Dimensional Isoenergetic Jet Mixing Zones." AEDC-TDR-63-253 (AD426116), December 1963.

APPENDIXES

- I. ILLUSTRATIONS**
- II. EQUATIONS FOR THE CHARACTERISTICS OF GENERAL,
SINGLE-STREAM MIXING ZONES**

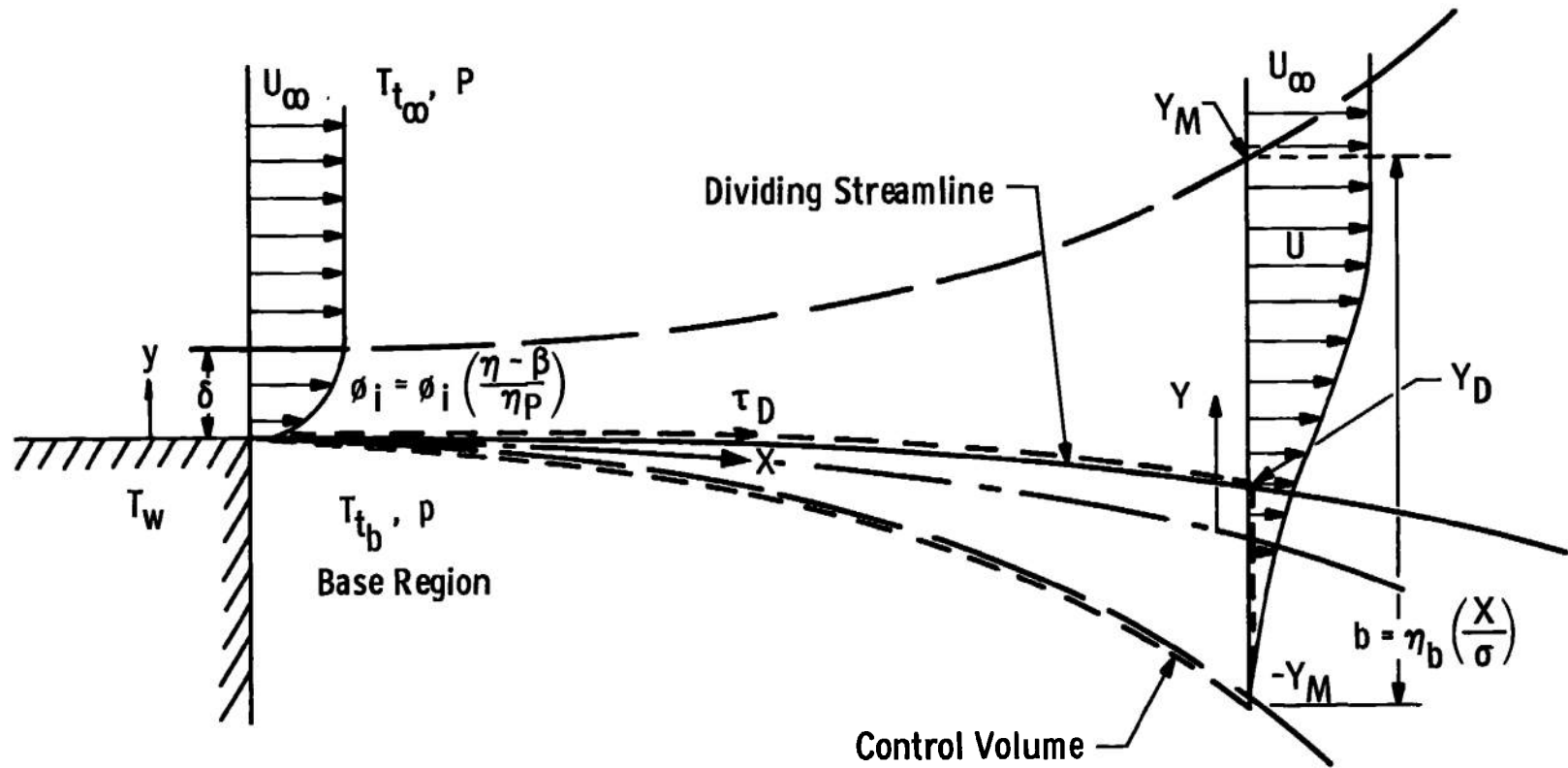


Fig. 1 General Mixing Zone

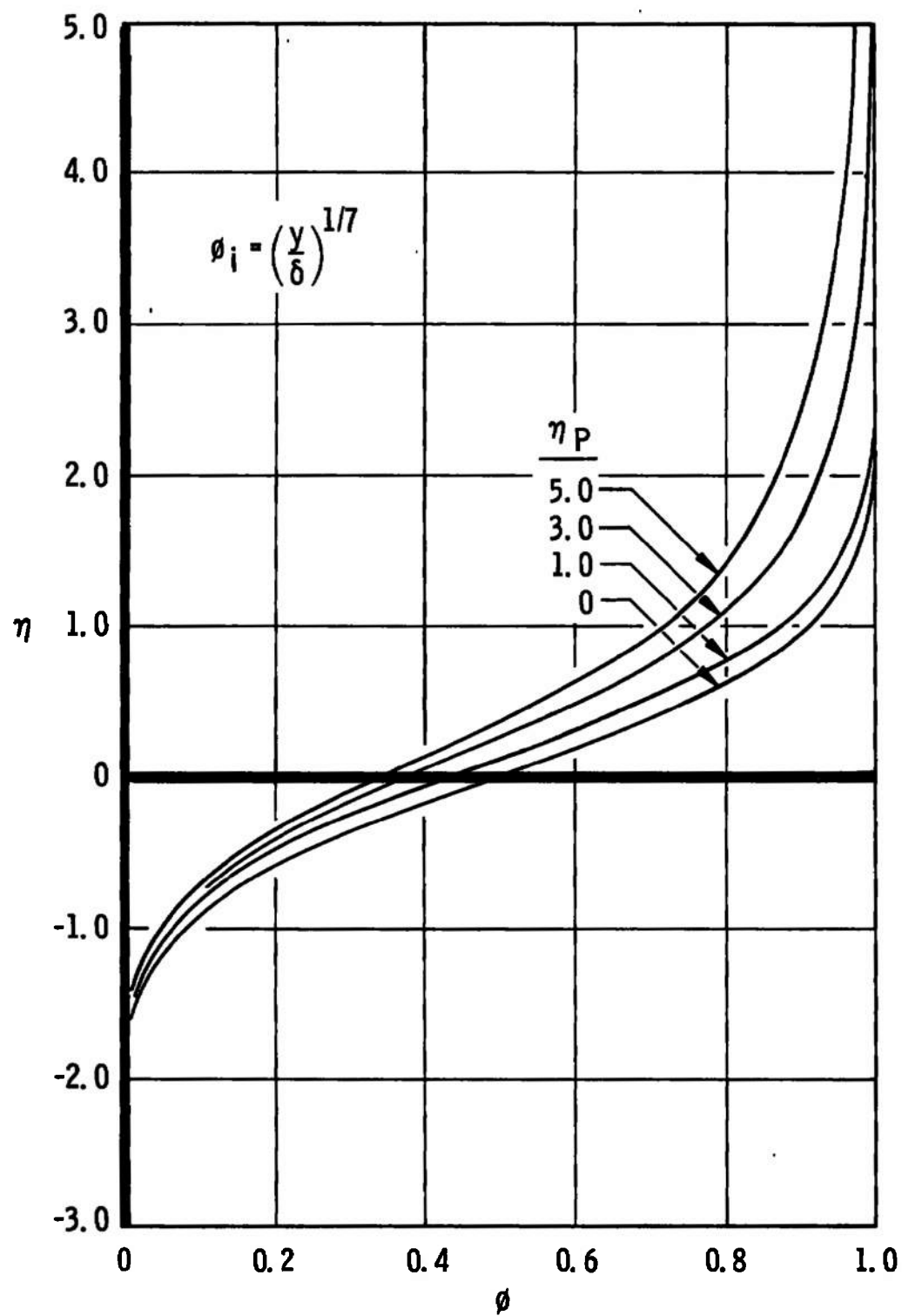
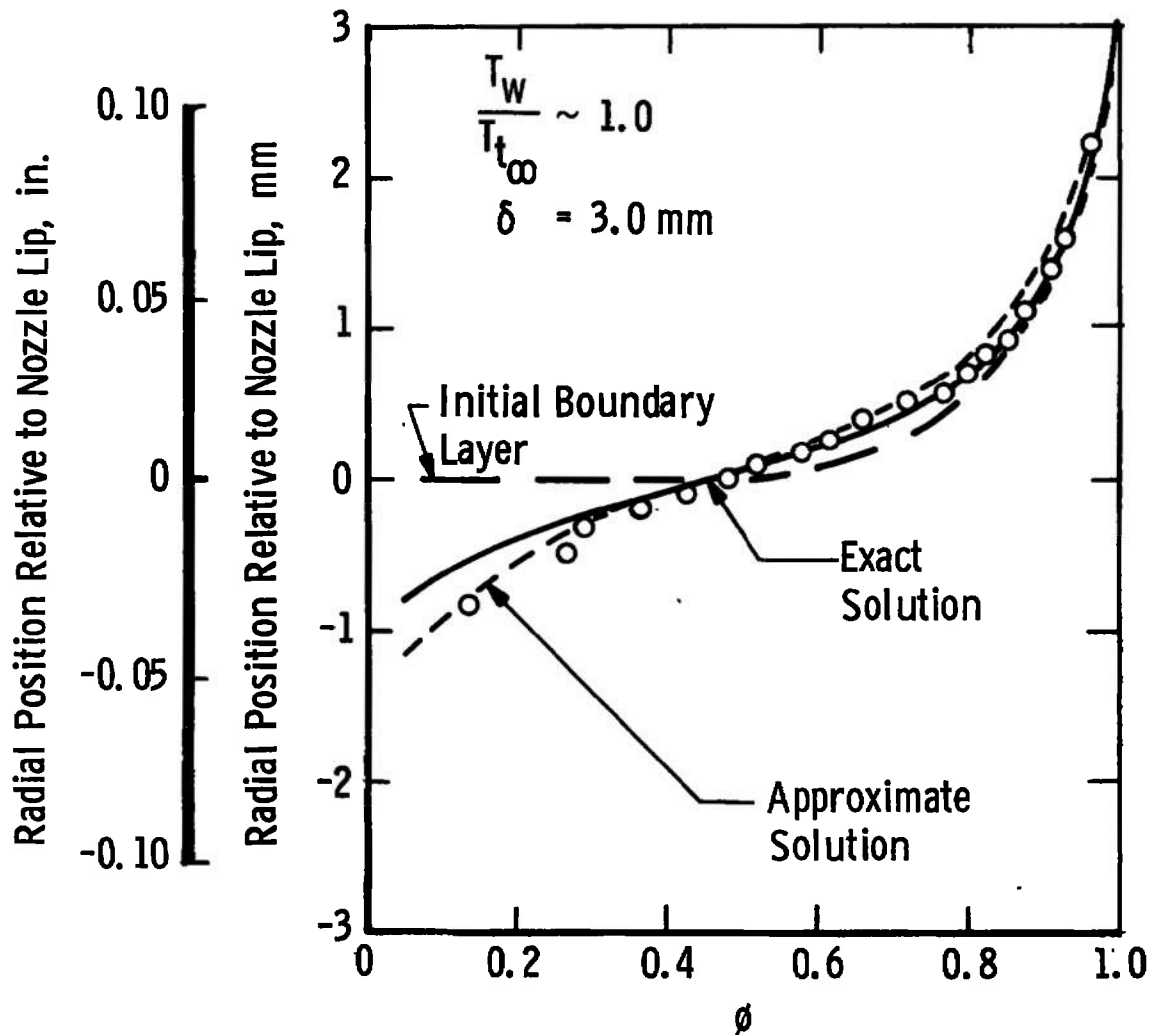
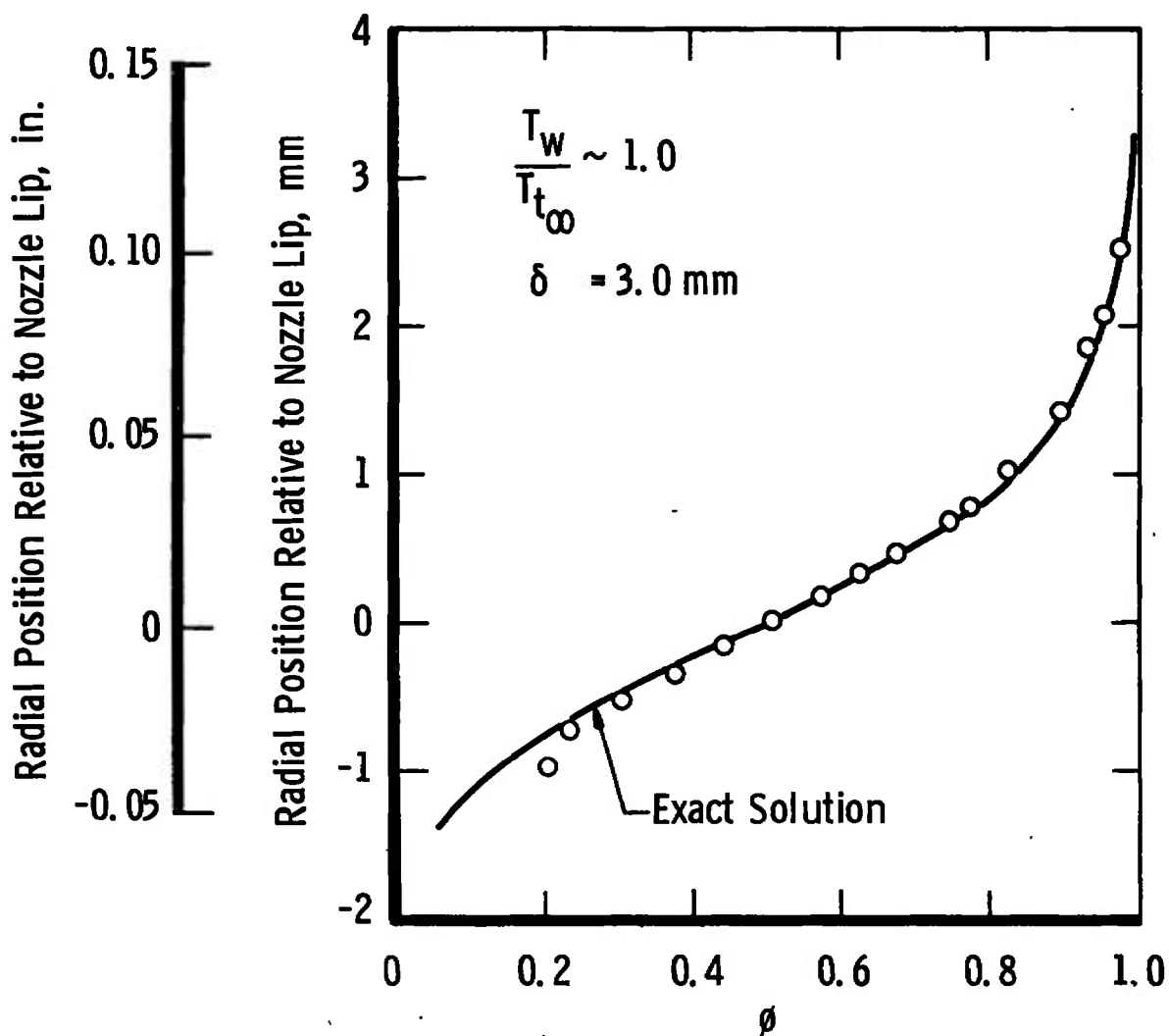


Fig. 2 Typical Family of Velocity Profiles

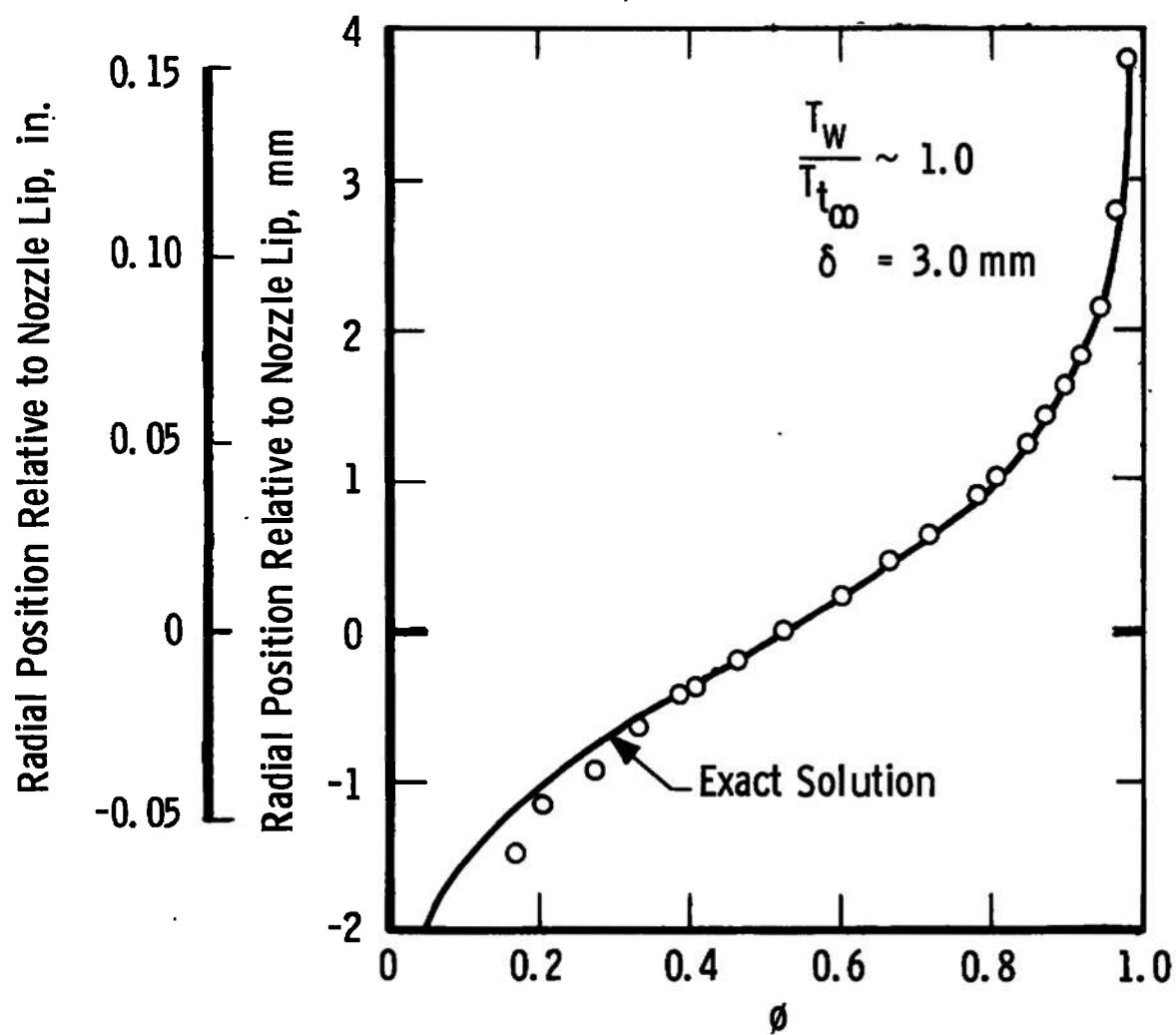


a. $\psi = 2.0$, $M_\infty = 0.19$

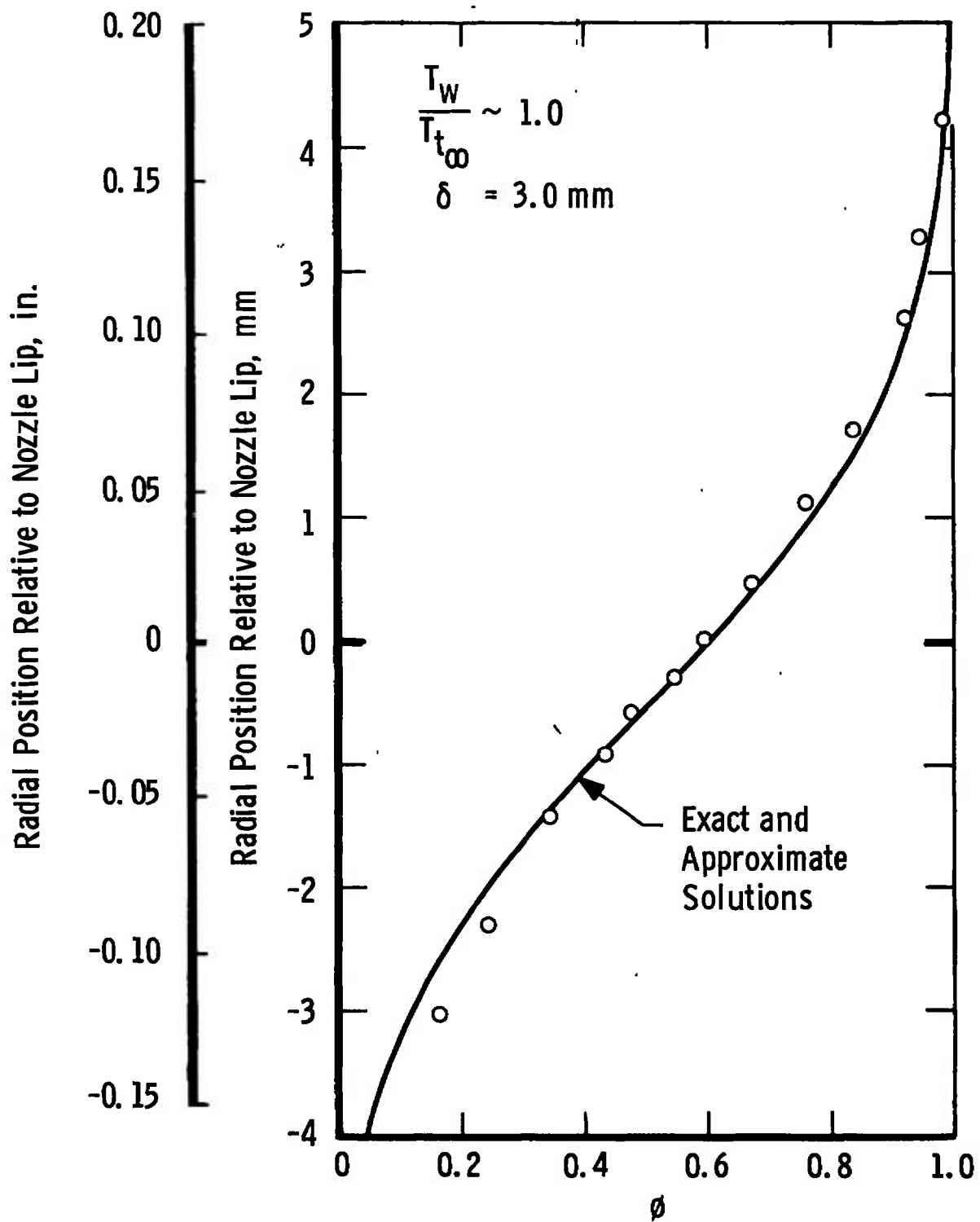
Fig. 3 Comparison of Theory and Chapman's Data



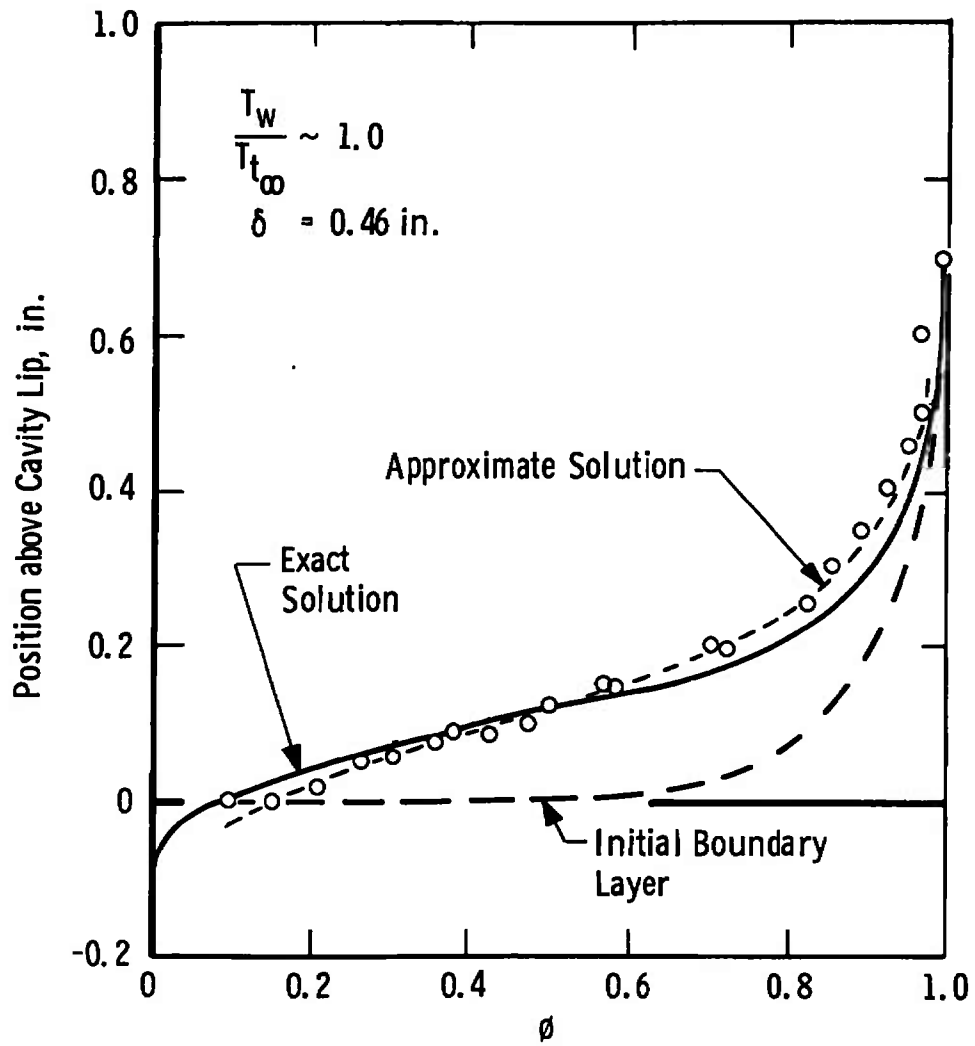
b. $\psi = 3.3, M_\infty = 0.19$
 Fig. 3 Continued



c. $\psi = 4.7, M_\infty = 0.19$
 Fig. 3 Continued

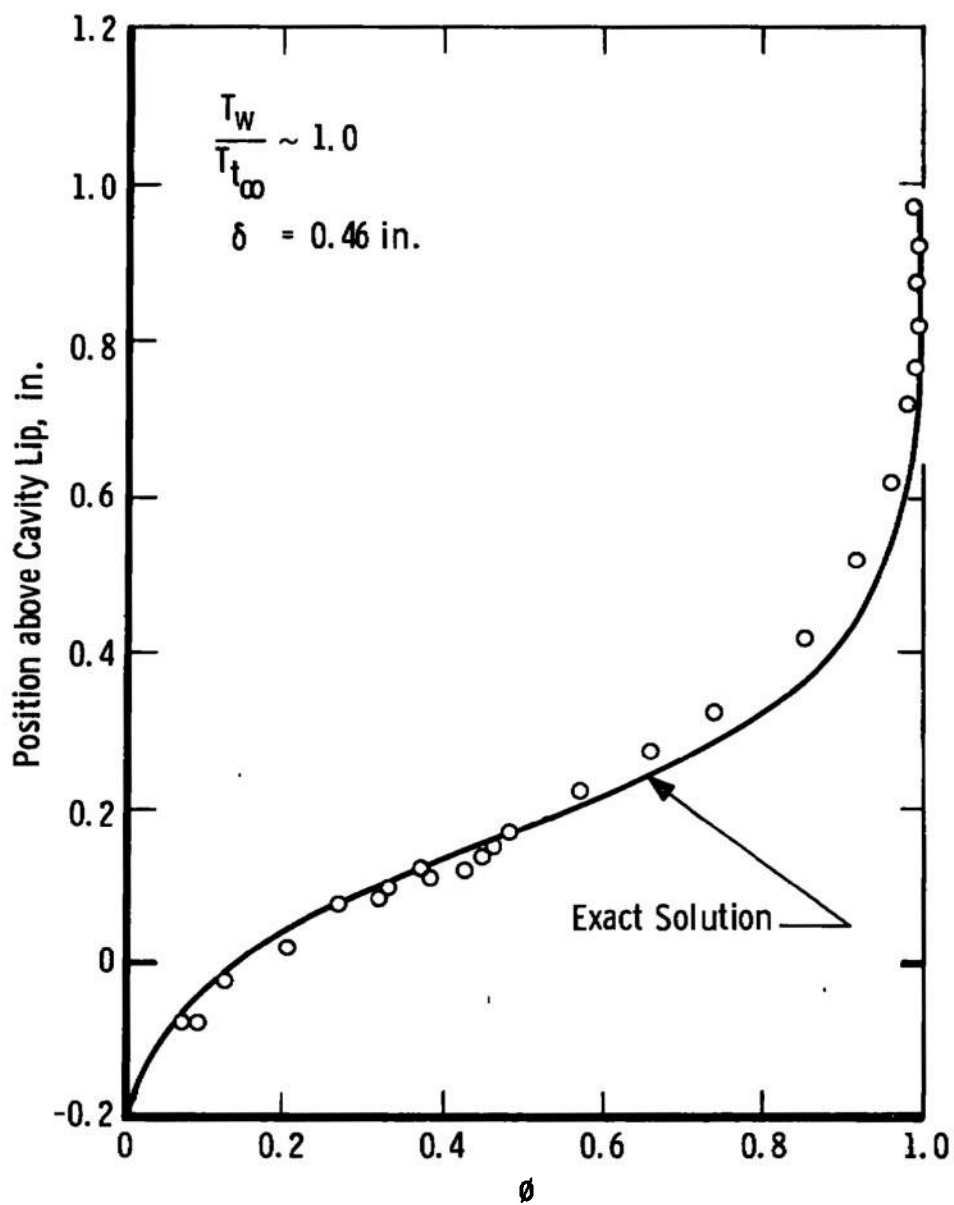


d. $\psi = 9.7$, $M_\infty = 0.19$
 Fig. 3 Concluded

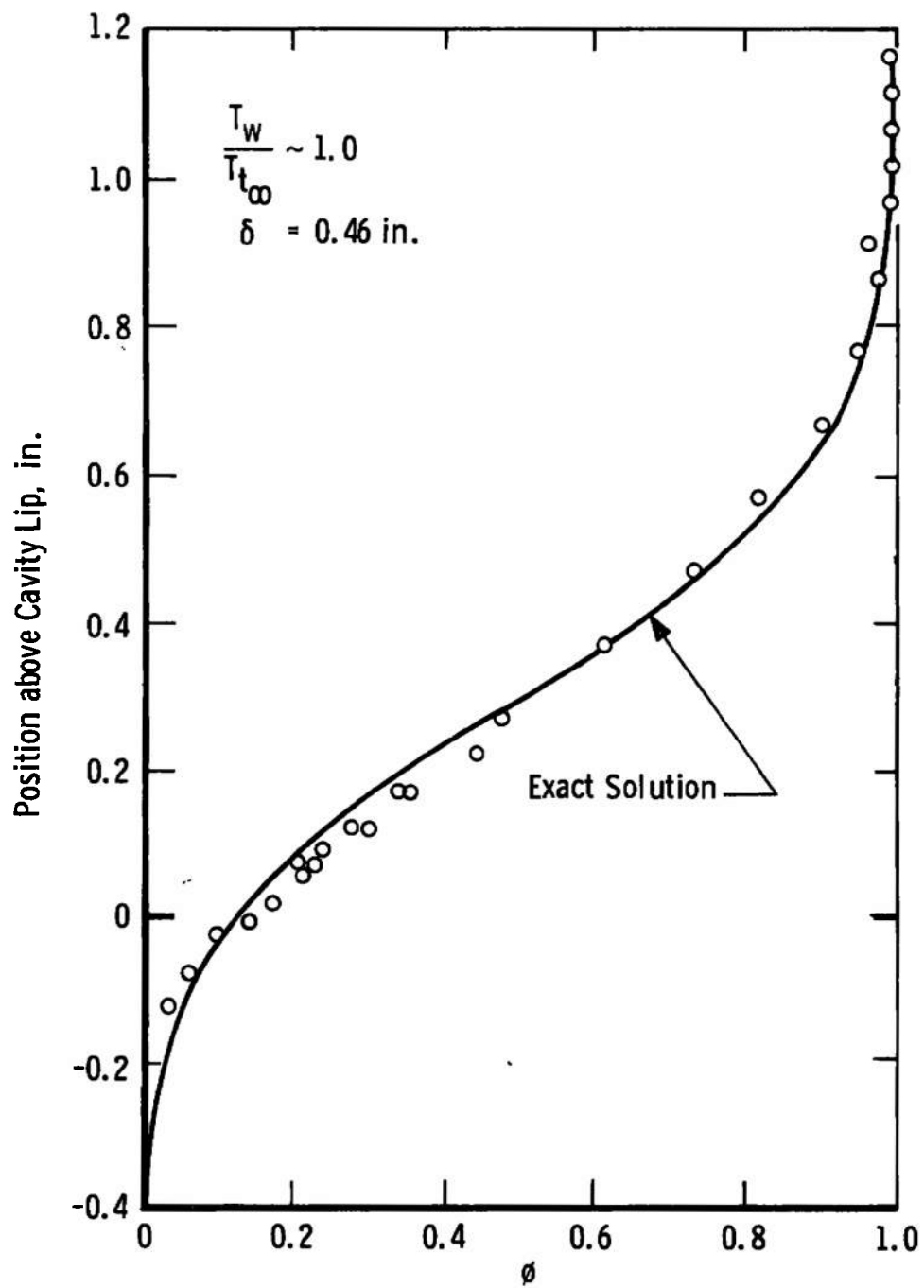


a. $\psi = 2.1, M_\infty = 2.1$

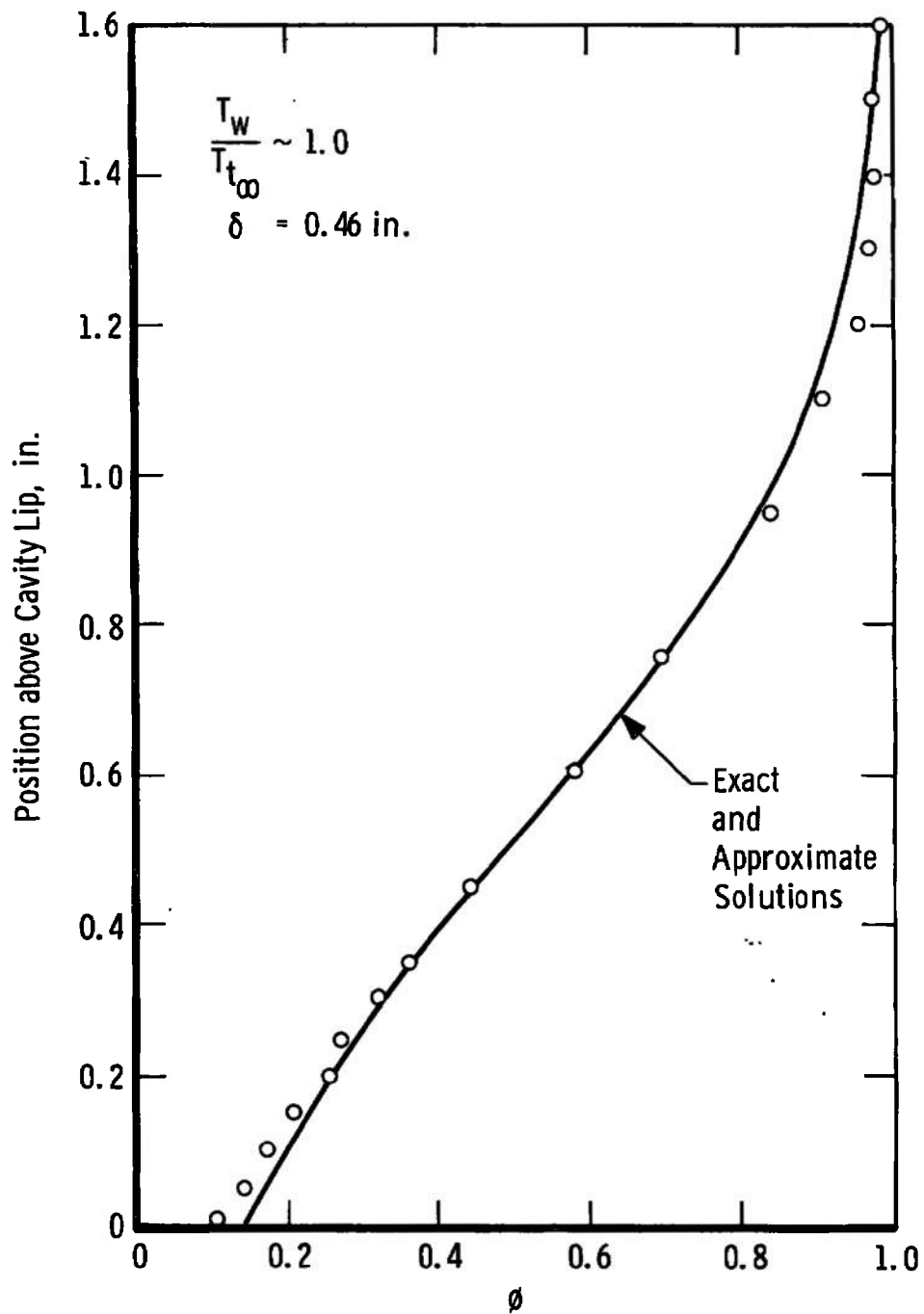
Fig. 4 Comparison of Theory and Hill's Data



b. $\psi = 4.6, M_\infty = 2.1$
Fig. 4 Continued

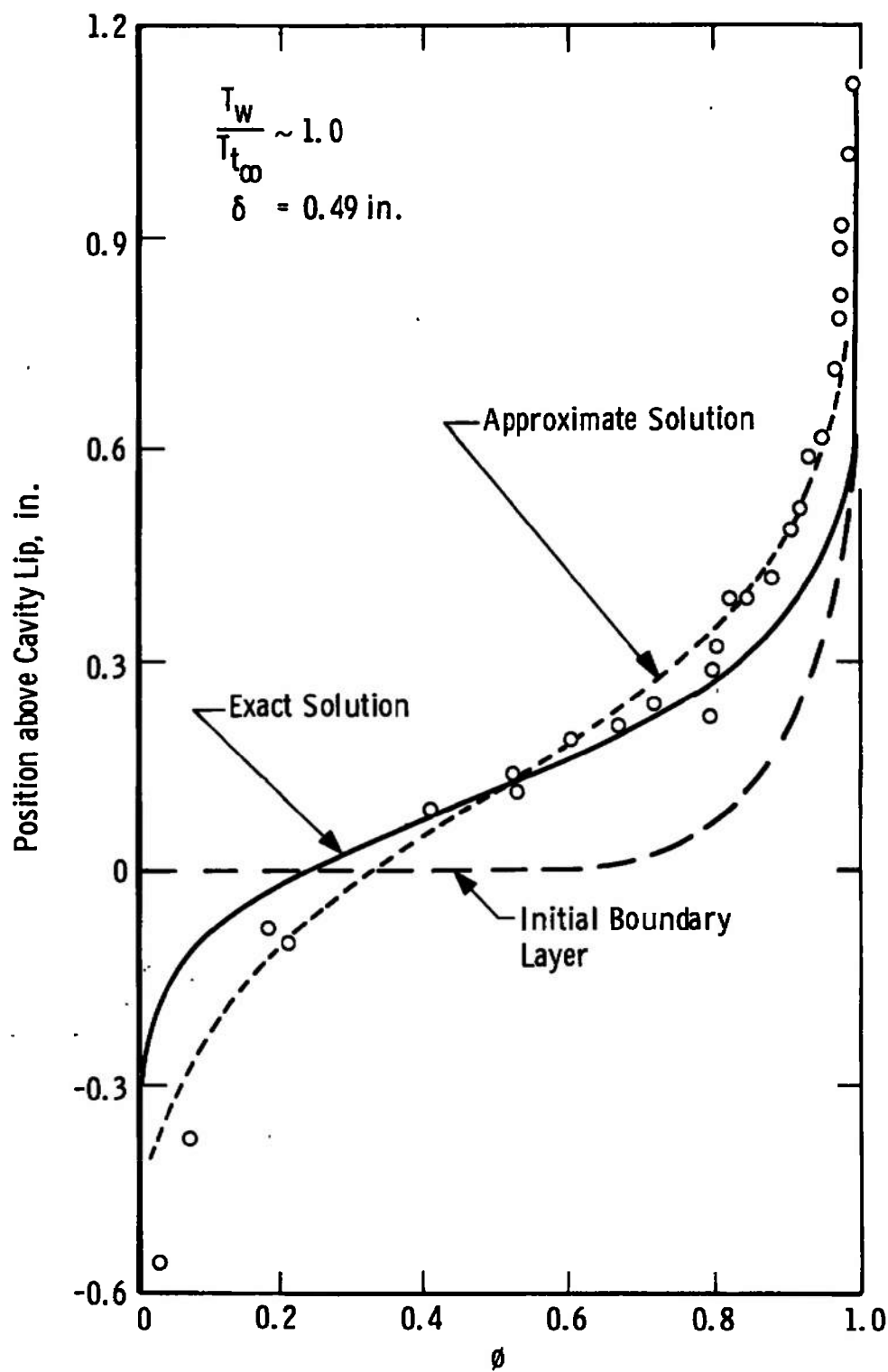


c. $\psi = 8.4, M_\infty = 2.1$
Fig. 4 Continued

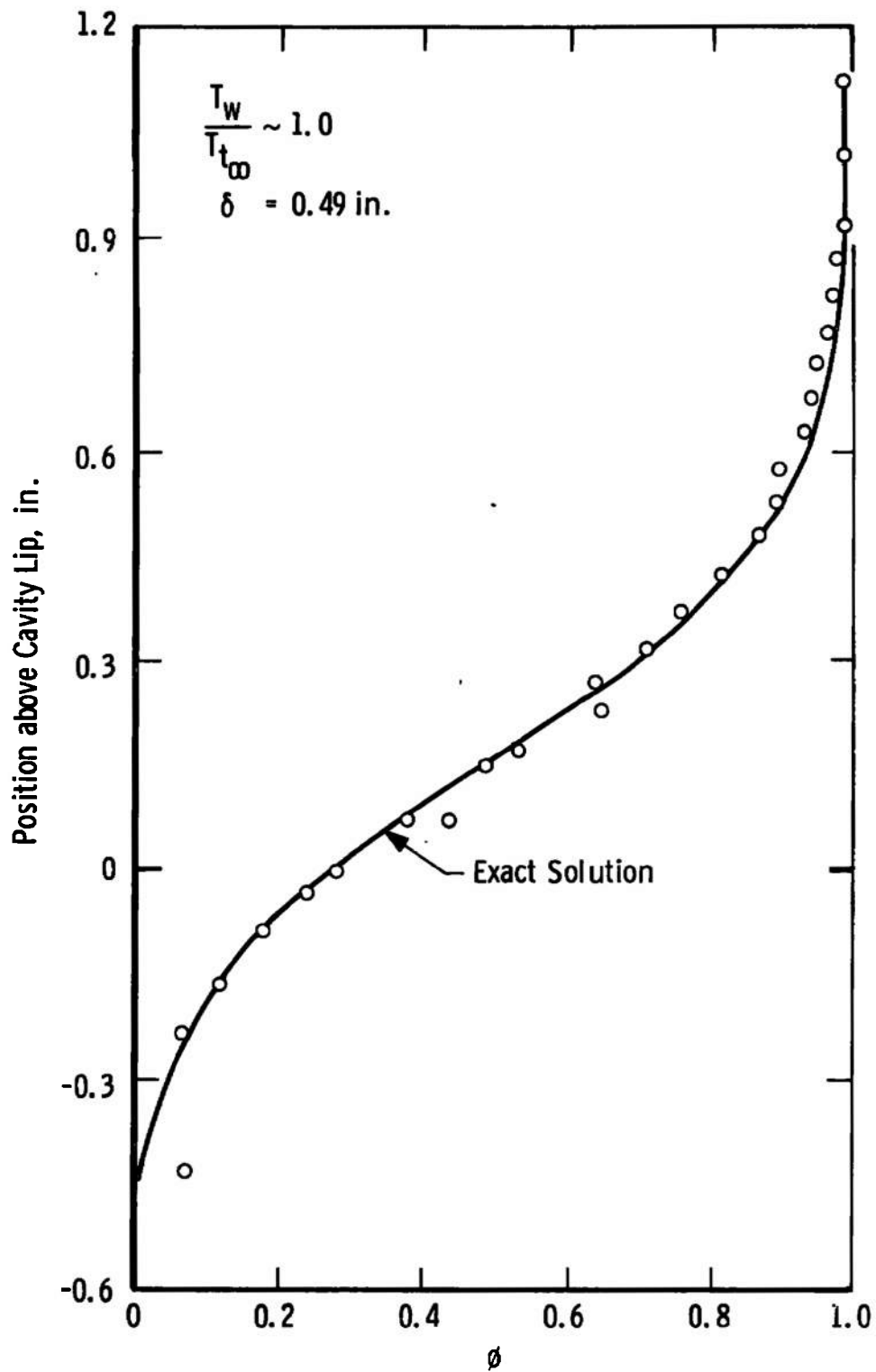


d. $\psi = 17.4, M_\infty = 2.1$

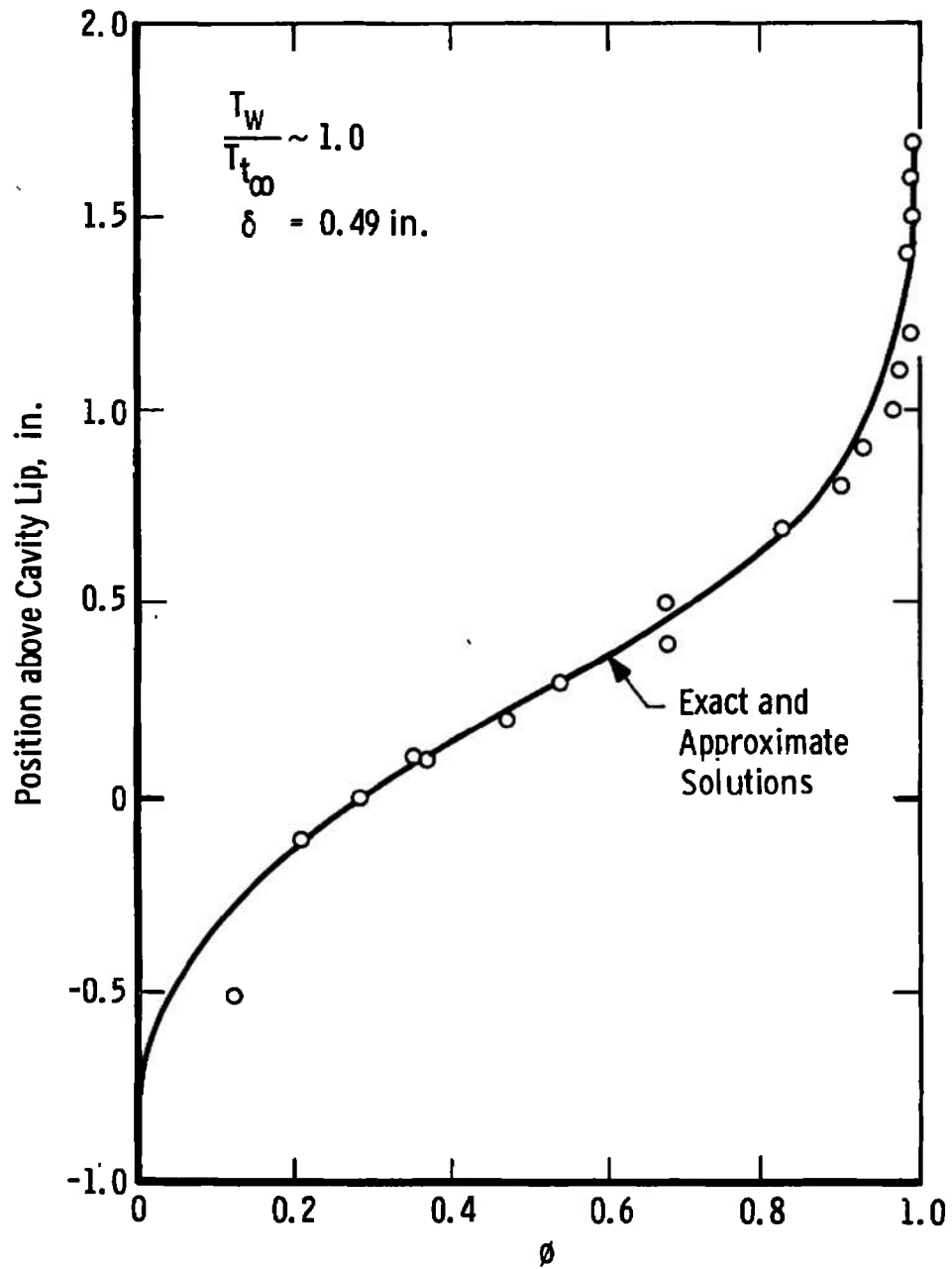
Fig. 4 Continued



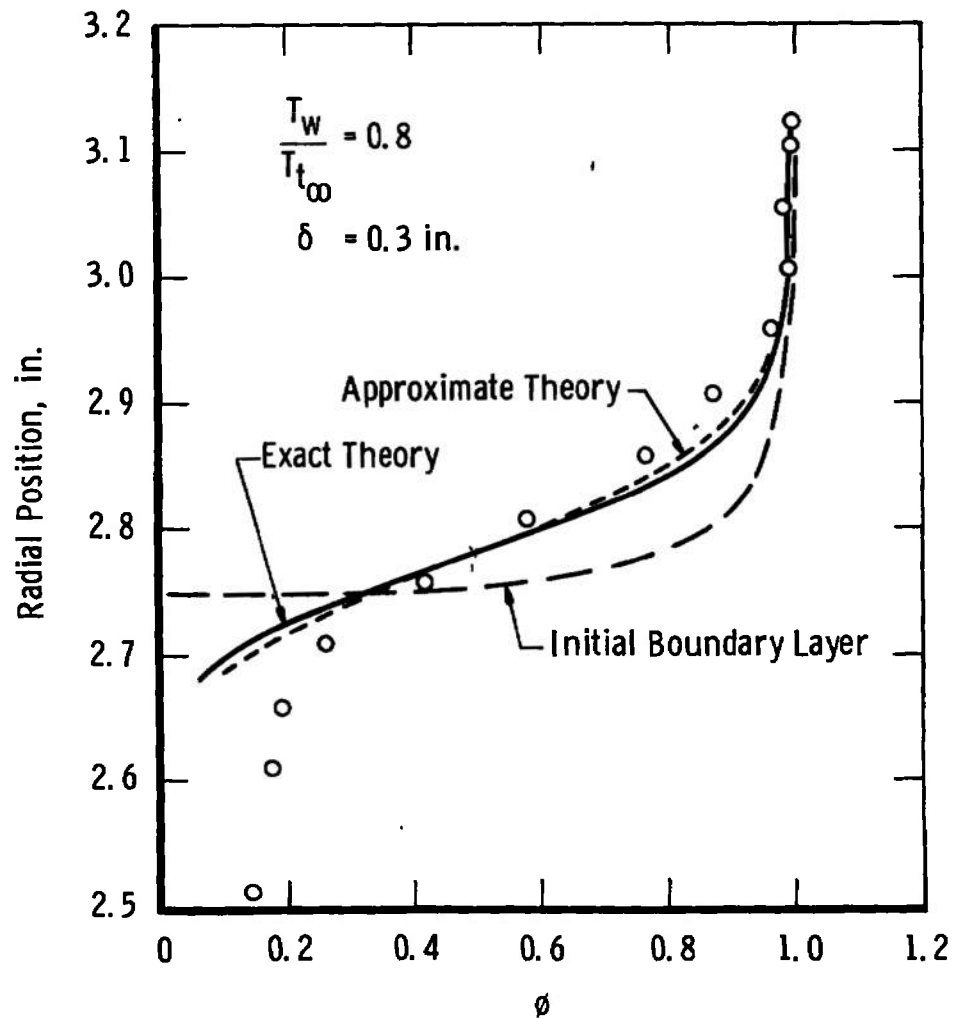
e. $\psi = 4.3$, $M_\infty = 2.5$
 Fig. 4 Continued



f. $\psi = 7.7, M_\infty = 2.5$
Fig. 4 Continued

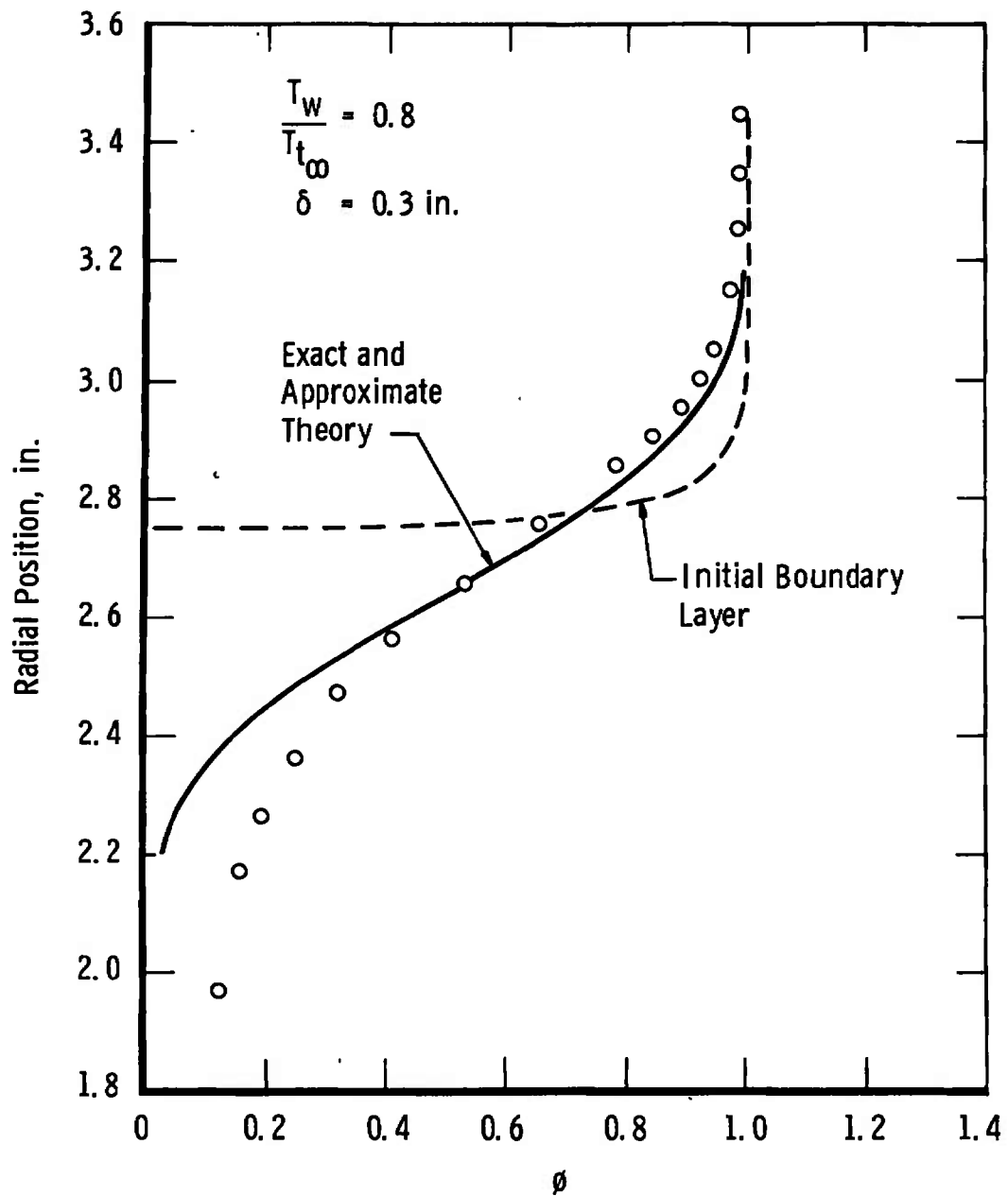


g. $\psi = 16.0, M_\infty = 2.5$
Fig. 4 Concluded

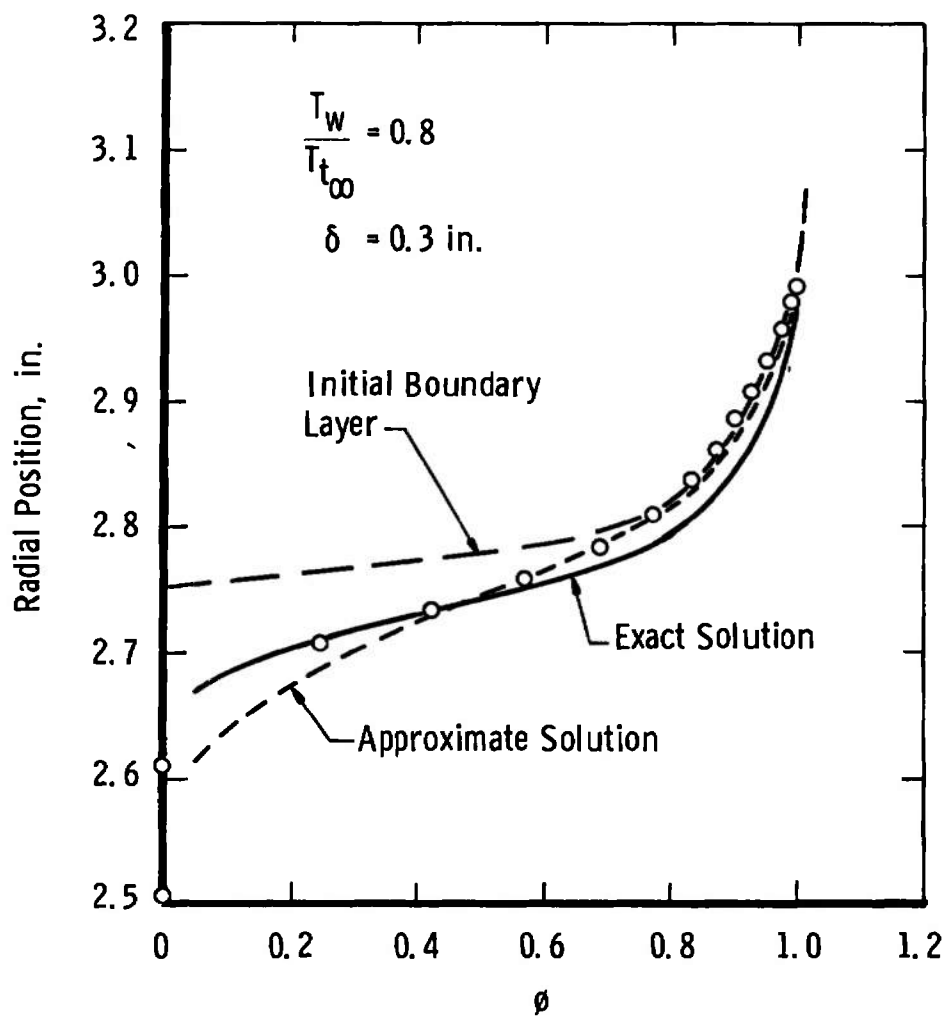


a. $\psi = 2.7, M_\infty = 4.0$

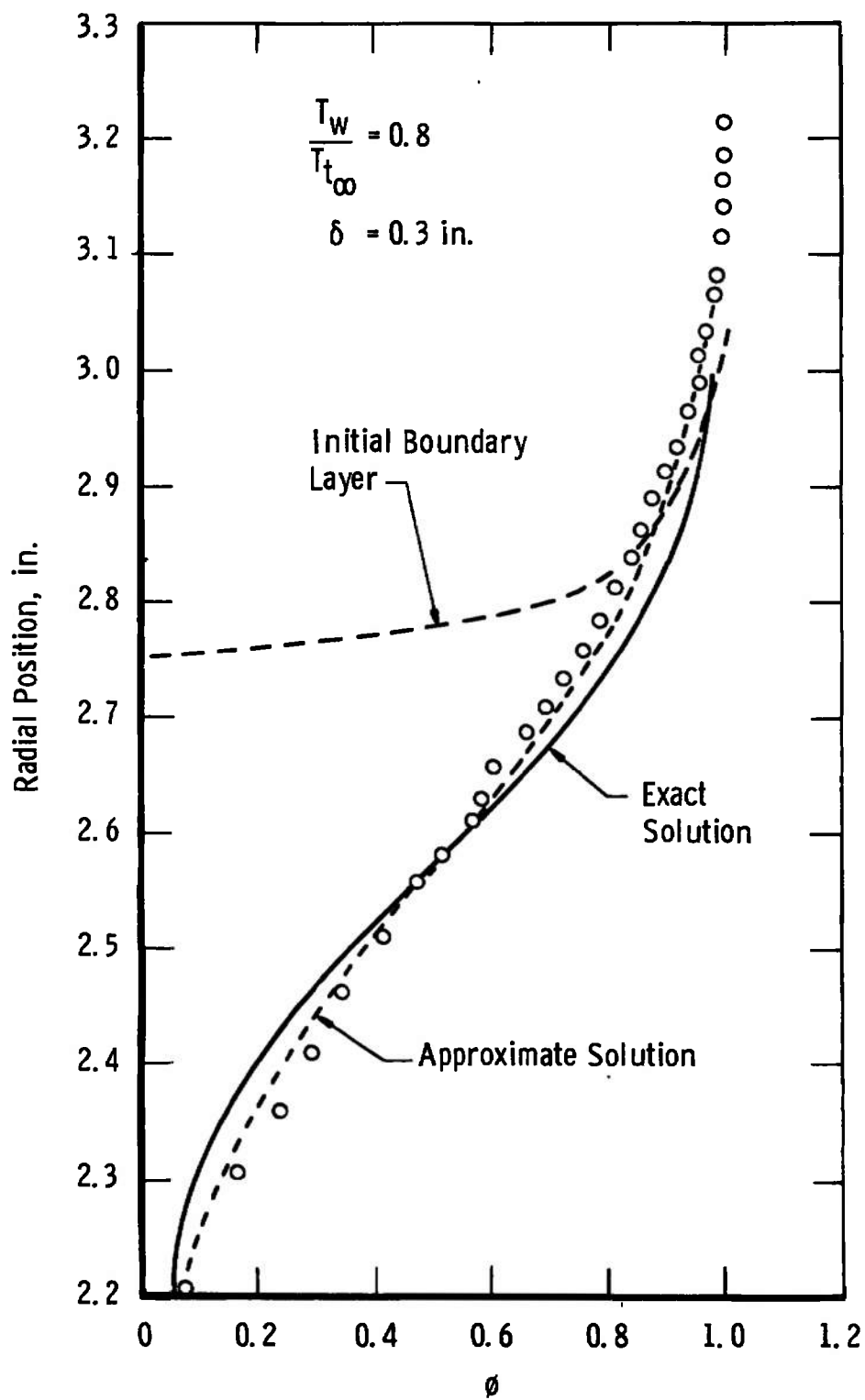
Fig. 5 Comparison of Theory and High-Speed Data from Ref. 9



b. $\psi = 13.3$, $M_\infty = 4.0$
Fig. 5 Continued



c. $\psi = 3.33$, $M_\infty = 6.4$
Fig. 5 Continued



d. $\psi = 15.8$, $M_\infty = 6.4$

Fig. 5 Concluded

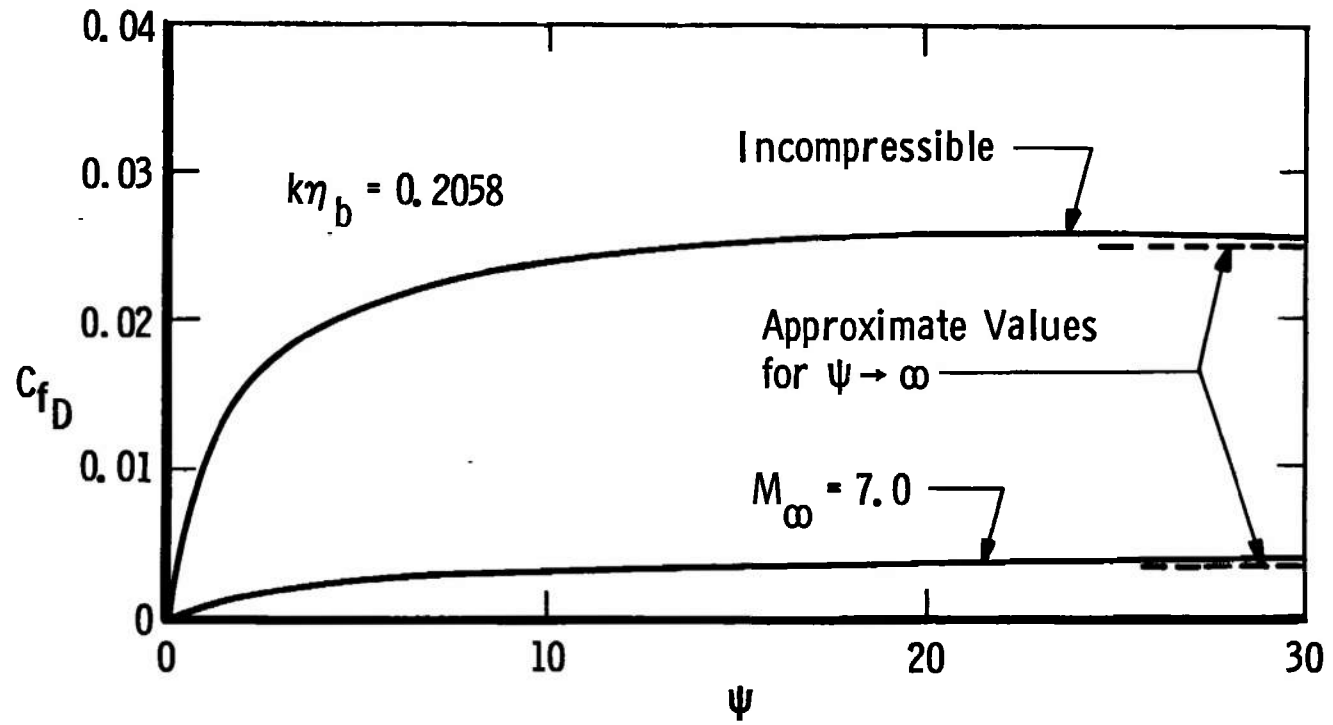


Fig. 6 Theoretical Variation of Dividing Streamline Friction Coefficient

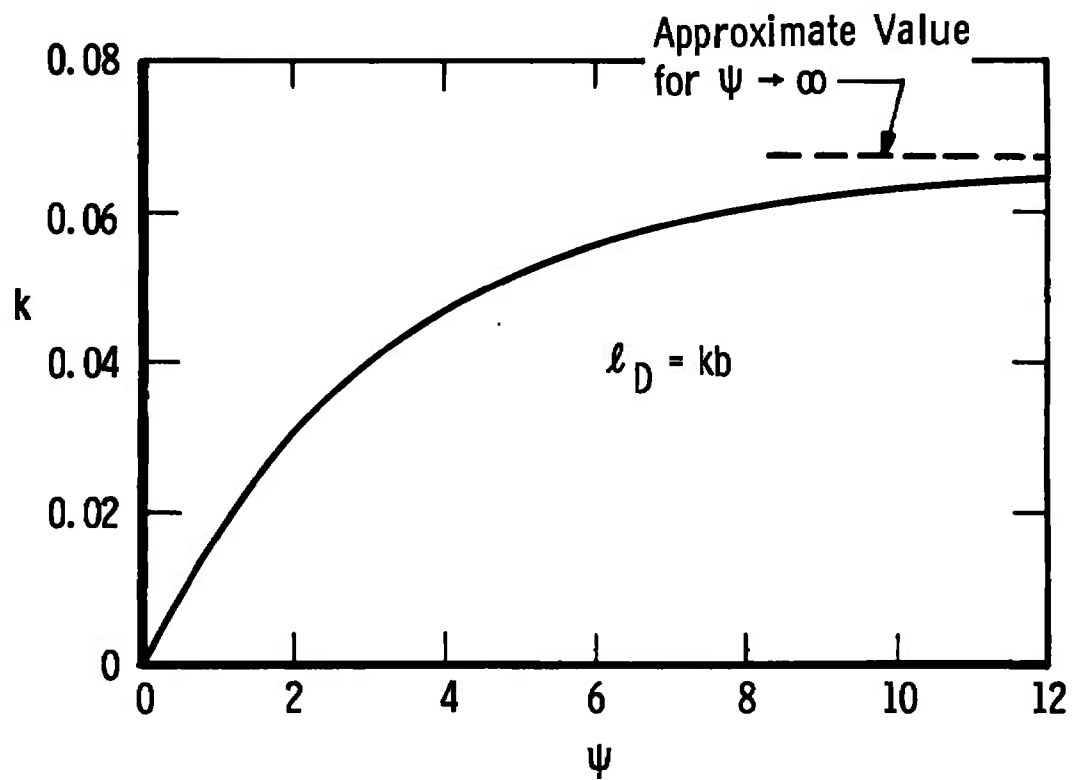
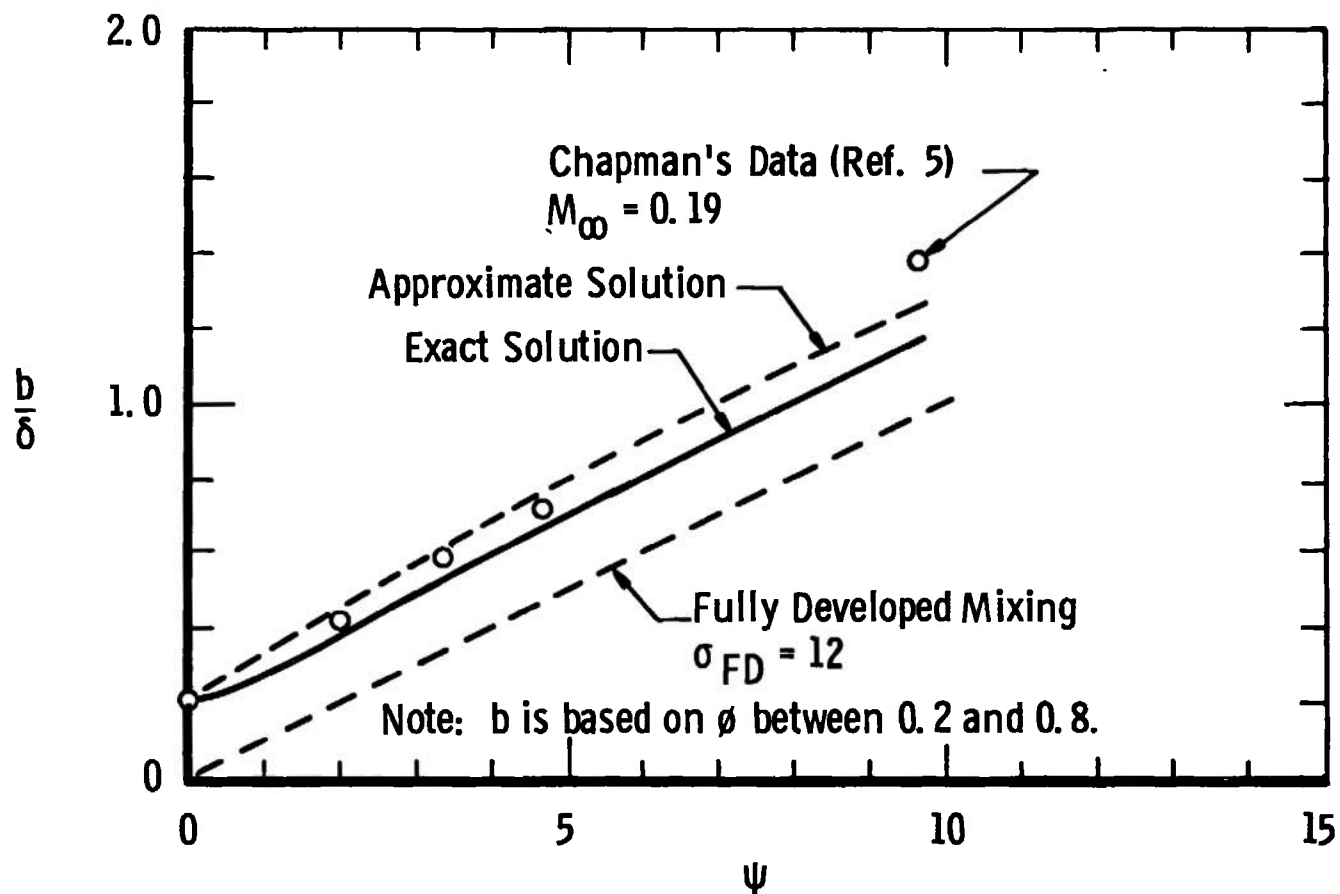
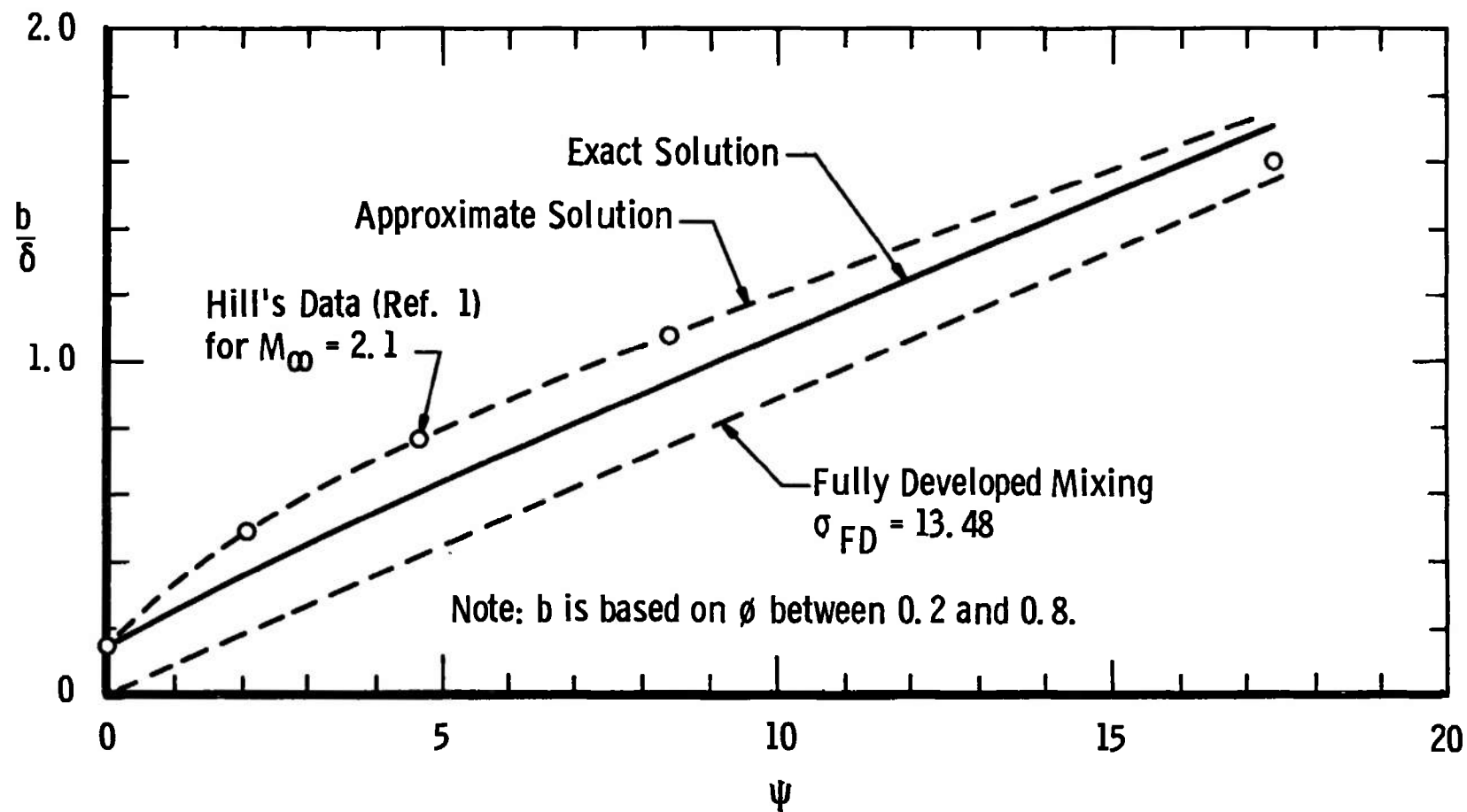


Fig. 7 Theoretical Variation of Mixing Length Proportionality Constant



a. With Chapman's Data
 Fig. 8 Comparison of Theoretical Mixing Growth



b. With Hill's Data
Fig. 8 Concluded

APPENDIX II

EQUATIONS FOR THE CHARACTERISTICS OF GENERAL, SINGLE-STREAM MIXING ZONES

Application of the Chapman-Korst flow model to base flow problems requires details of the associated mixing zone and its location with respect to the corresponding inviscid jet. The mixing zone is located by the requirement that the momentum flux in the actual viscous case is identical to the momentum flux of the corresponding inviscid jet. With a specification of the property variations in the mixing zone, continuity requirements can be used to locate the dividing streamline between the jet flow and the fluid entrained from the surroundings. Zumwalt (Ref. 11) first derived the relationships for the axisymmetric mixing zone characteristics in conjunction with his analysis of the base pressure problem. These relationships were rederived by the authors from a more general approach, and the results have been reapplied to the cases treated by Zumwalt.

ANALYSIS

The present analysis is simply based on the dividing streamline and corresponding inviscid jet boundary definitions and the realization that these are local characteristics relating the actual viscous case to a corresponding inviscid jet. Concepts inherent to the analysis can be demonstrated by considering a general control volume that is everywhere exterior to the mixing zone except at the point (station 3, Fig. II-1, for example) in question. If steady conditions prevail and base region velocities are negligible, it is evident that forces on the upstream portion of the control volume in the actual case must be identical to the upstream forces on the same control volume superimposed on the corresponding inviscid jet. Therefore, at the point where mixing zone characteristics are desired,

$$F_{3I} \left| \begin{array}{c} Y_{M3} \\ -Y_{M3} \end{array} \right. = F_{3V} \left| \begin{array}{c} Y_{M3} \\ -Y_{M3} \end{array} \right. \quad (\text{II-1})$$

Application of mass conservation to the same control volume for the actual viscous case and for a corresponding inviscid jet yields

$$G_{3I} \left| \begin{array}{c} Y_{M3} \\ Y_{m3} \end{array} \right. = G_{3V} \left| \begin{array}{c} Y_{M3} \\ Y_{D3} \end{array} \right. \quad (\text{II-2})$$

APPLICATIONS

Zumwalt's most general analysis involves an "externally expanding" flow field similar to that shown in Fig. II-1 without an initial boundary layer. Pressure gradients were considered in the streamwise direction, but uniform transverse static pressure conditions were assumed to exist at each station. Application of the present analysis to this flow field yields

$$F_{3V} \Big|_{-Y_{M3}}^{Y_{M3}} = \int_{-Y_{M3}}^{Y_{M3}} \rho_{3V} u_{3V}^2 2\pi \left[r_s + (Y - Y_{m3}) \cos \theta_s + r_s + (Y - Y_{m3} + dY) \cos \theta_s \right] \frac{dY}{2} \\ + 2\pi p_s \left(\frac{2Y_{M3}}{2} \right) \left[r_s - (Y_{M3} + Y_{m3}) \cos \theta_s + r_s + (Y_{M3} - Y_{m3}) \cos \theta_s \right] \quad (\text{II-3})$$

and

$$G_{3V} \Big|_{Y_{D3}}^{Y_{M3}} = \int_{Y_{D3}}^{Y_{M3}} \rho_{3V} u_{3V} 2\pi \left[r_s + (Y - Y_{m3}) \cos \theta_s + r_s + (Y - Y_{m3} + dY) \cos \theta_s \right] \frac{dY}{2} \quad (\text{II-4})$$

for the actual viscous case and

$$F_{3I} \Big|_{-Y_{M3}}^{Y_{M3}} = \rho_{3I} u_{3I}^2 2\pi \left(\frac{Y_{M3} - Y_{m3}}{2} \right) \left[r_s + r_s + (Y_{M3} - Y_{m3}) \cos \theta_s \right] \\ + 2\pi p_s \left(\frac{2Y_{M3}}{2} \right) \left[r_s - (Y_{M3} + Y_{m3}) \cos \theta_s + r_s + (Y_{M3} - Y_{m3}) \cos \theta_s \right] \quad (\text{II-5})$$

and

$$G_{3I} \Big|_{Y_{m3}}^{Y_{M3}} = \rho_{3I} u_{3I} 2\pi \left(\frac{Y_{M3} - Y_{m3}}{2} \right) \left[r_s + r_s + (Y_{M3} - Y_{m3}) \cos \theta_s \right] \quad (\text{II-6})$$

for the corresponding inviscid jet.

Substituting into Eqs. (II-1) and (II-2) and non-dimensionalizing the results yield

$$(\eta_{M3} - B_1)^2 + 2(1 - C_{3I}^2) \left[(I_1)_{\eta_{M3}} - (I_1)_{\eta_{D3}} \right] B_1 - 2(1 - C_{3I}^2) \left[(J_1)_{\eta_{M3}} - (J_1)_{\eta_{D3}} \right] = \left(\frac{\sigma r_s}{X \cos \theta_s} \right)^2 \quad (\text{II-7})$$

and

$$\eta_{m3} = B_1 + \frac{\sigma r_s}{X \cos \theta_s} \quad (\text{II-8})$$

where

$$B_1 = \frac{[(J_1)\eta_{D3} - (J_1)\eta_{M3} + (J_3)\eta_{M3}]}{[(I_1)\eta_{D3} - (I_1)\eta_{M3} + (I_3)\eta_{M3}]}$$

Zumwalt's results, which are based on a more restrictive control volume specification, are

$$(B - \eta_{M3})^2 + 2(1 - C_{3I})[(I_1)\eta_{M3} - (I_1)\eta_{D3}]B - 2(1 - C_{3I})[(J_1)\eta_{M3} - (J_1)\eta_{D3}] = \left(\frac{\sigma r_3}{X \cos \theta_3}\right)^2 \quad (\text{II-9})$$

and

$$\eta_{m3} = B + \frac{\sigma r_3}{X \cos \theta_3} \quad (\text{II-10})$$

where

$$B = \frac{(J_1)\eta_{D3} - \left(1 - \frac{C_{3I}}{C_{2I}}\right)(J_1)\eta_{M3} - \left(\frac{C_{3I}}{C_{2I}}\right)[(J_1)\eta_{M3} - (J_3)\eta_{M3}]}{(I_1)\eta_{D3} - \left(1 - \frac{C_{3I}}{C_{2I}}\right)(I_1)\eta_{M3} - \left(\frac{C_{3I}}{C_{2I}}\right)[(I_1)\eta_{M3} - (I_3)\eta_{M3}] + \left(\frac{\gamma-1}{\gamma}\right)\left(\frac{\eta_{M3}}{C_{2I}C_{3I}}\right)\left(1 - \frac{P_b}{P_3}\right)}$$

Although the equation forms are similar, Zumwalt's results differ from the present analysis because upstream flow conditions, base pressure, and specific heat ratio are involved in B , whereas B_1 is independent of these parameters. The effect of this difference on the dividing streamline velocity ratio, for example, and the relationship to the two-dimensional result are illustrated in Fig. II-2. Note that ϕ_{D3} computed by the present analysis approaches the two-dimensional value as the geometric parameter approaches infinity, which is intuitively expected.

For the special case of uniform flow, static pressure is also constant in the streamwise direction, and $C_{2I} = C_{3I}$. Under these conditions, $B = B_1$, and Zumwalt's results agree with the present analysis.

Equations (II-7) and (II-8) are also applicable to the problem of internally expanding jets (i. e., converging-diverging nozzle exit flows) if the sign of r_3 is changed. Under these circumstances, uniform flow conditions exist along the jet boundary, and the present analysis is once again in agreement with Zumwalt.

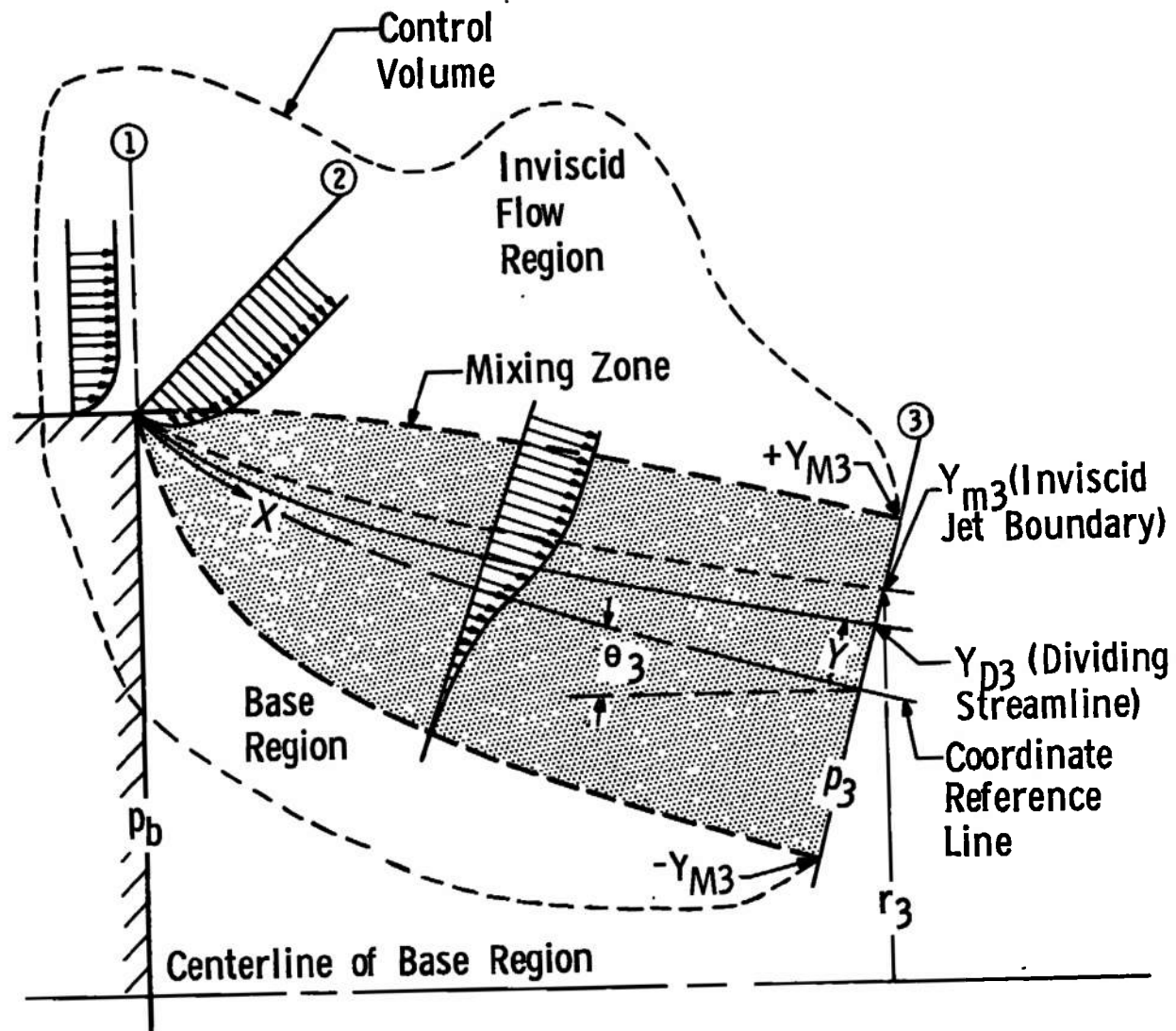


Fig. II-1 General Mixing Zone

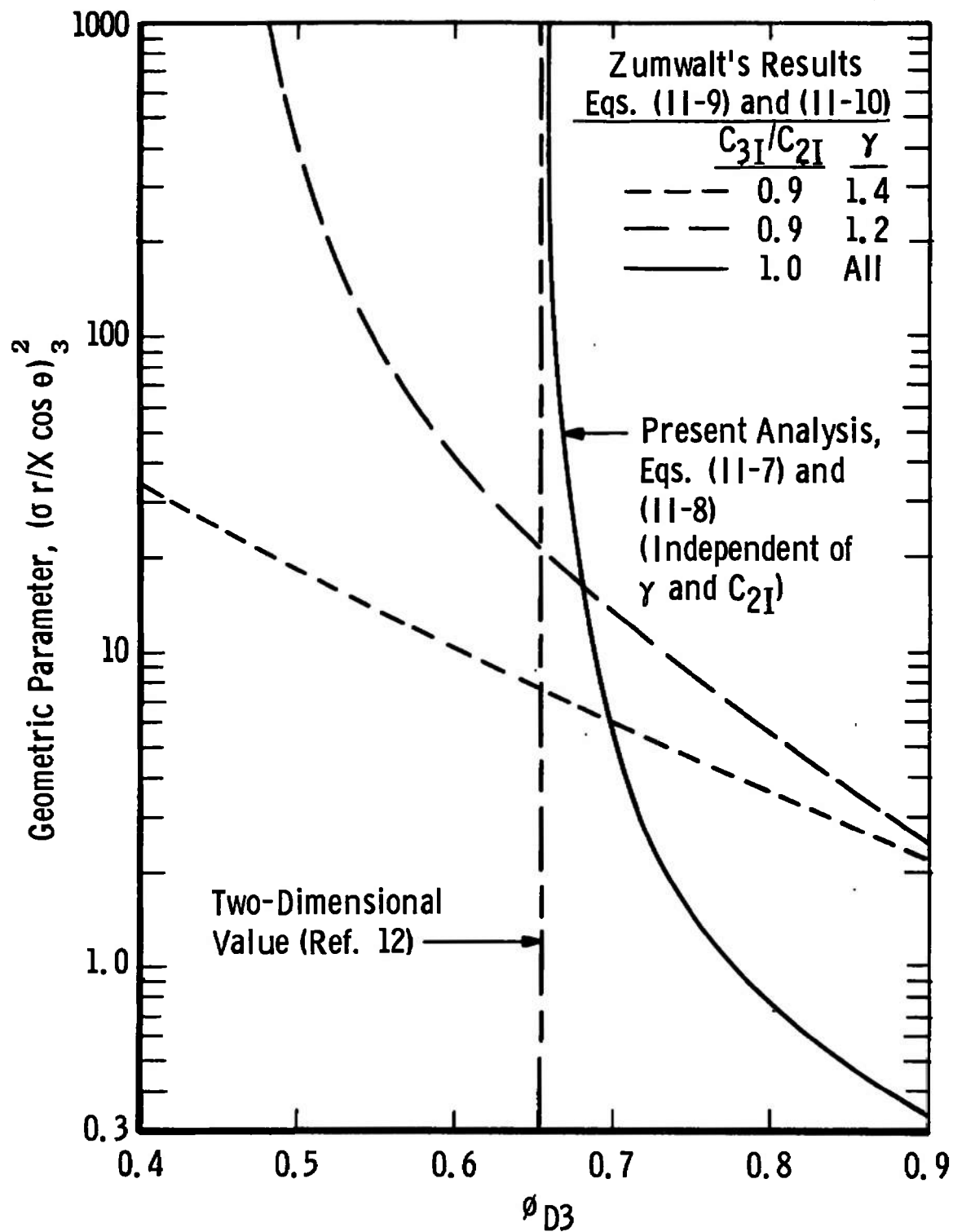


Fig. II-1 Variation of Dividing Streamline Velocity Ratio

DOCUMENT CONTROL DATA - R & D

(Security classification of title, body of abstract and indexing annotation must be entered when the overall report is classified)

1. ORIGINATING ACTIVITY (Corporate author) Arnold Engineering Development Center, ARO, Inc., Operating Contractor, Arnold Air Force Station, Tennessee 37389		2a. REPORT SECURITY CLASSIFICATION UNCLASSIFIED	
		2b. GROUP N/A	
3. REPORT TITLE INFLUENCE OF INITIAL BOUNDARY LAYER ON THE TWO-DIMENSIONAL TURBULENT MIXING OF A SINGLE STREAM			
4. DESCRIPTIVE NOTES (Type of report and inclusive dates) July 1, 1969, to June 30, 1970--Final Report			
5. AUTHOR(S) (First name, middle initial, last name) R. C. Bauer and R. J. Matz, ARO, Inc.			
6. REPORT DATE April 1971		7a. TOTAL NO. OF PAGES 46	7b. NO. OF REFS 12
8a. CONTRACT OR GRANT NO. F40600-71-C-0002		9a. ORIGINATOR'S REPORT NUMBER(S) AEDC-TR-71-79	
b. PROJECT NO. 5730			
c. Program Element 62302F		9b. OTHER REPORT NO(S) (Any other numbers that may be assigned this report) ARO-ETF-TR-71-22	
d.			
10. DISTRIBUTION STATEMENT Approved for public release; distribution unlimited.			
11. SUPPLEMENTARY NOTES Available in DDC		12. SPONSORING MILITARY ACTIVITY Arnold Engineering Development Center (XON), Arnold Air Force Station, Tennessee 37389	

13. ABSTRACT

An integral method is presented for estimating the influence of an initial boundary layer on the development of a two-dimensional, isobaric, turbulent, free shear layer. The basic equation is derived by applying the principle that, at any streamwise station along the free shear layer, the momentum of the entrained flow equals the total axial turbulent shear force acting along the dividing streamline. This equation is solved using a single parameter family of velocity profiles derived by Korst and Prandtl's mixing length concept for turbulent shear stress. The theory involves one empirical constant which was evaluated using Tollmien's experimental data for incompressible, turbulent mixing. The theory is verified by comparing with experimental data for free-stream Mach numbers up to 6.4

14. KEY WORDS	LINK A		LINK B		LINK C	
	ROLE	WT	ROLE	WT	ROLE	WT
free shear layer development boundary layer separation mixing boundary layer flow two-dimensional flow turbulent flow laminar flow shear flow.						